

Hanna Stoll

Hanne Schistad Robak

Metabolic biomarkers and reactive stroma grading in human prostate cancer tissue

Student thesis in Medicine

Trondheim, November 2015

Supervisor: May-Britt Tessem

Co-supervisor: Tone F. Bathen

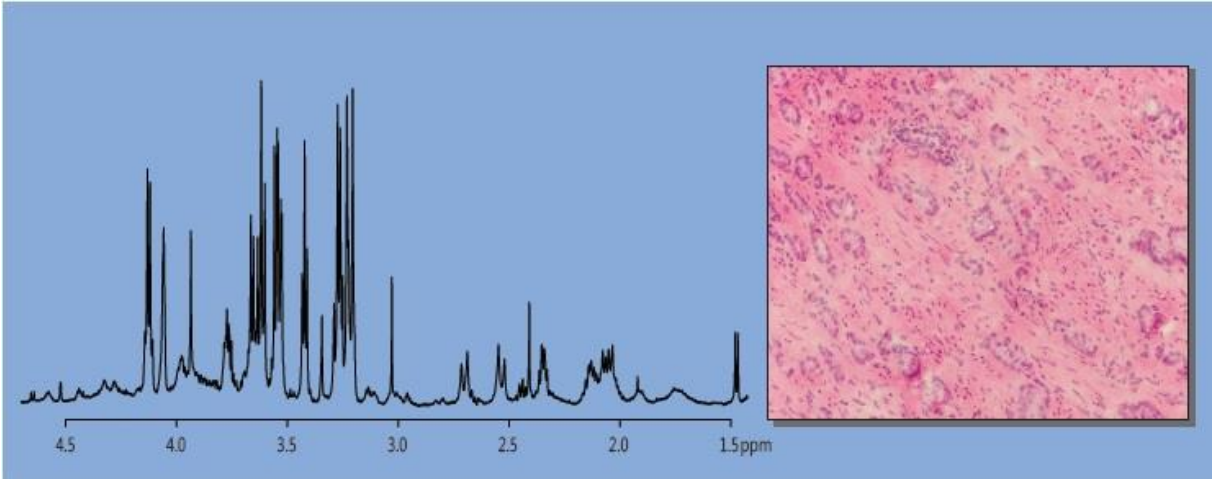
Norwegian University of Science and Technology

Faculty of Medicine

Department of Circulation and Medical Imaging (ISB)

Cover illustration:

The picture to the left shows an average metabolic spectrum of tissue samples containing stromogenic cancer (reactive stroma grade 3). To the the right is an example of the histological apparence of stromogenic cancer can be viewed.



Abstract

Introduction

Prostate cancer (PCa) is the most common malignancy among men in the western world. Today's diagnostic methods are not able to separate aggressive and indolent cancer in a sufficient way. Hence, it is difficult to choose which patients who will benefit from active surveillance, and which patients should receive active treatment. The purpose of our study was to reveal more information about metabolic pathways in PCa by combining two novel and emerging diagnostic methods: reactive stroma (RS), the interaction between cancer stroma and epithelium, and metabolic profiling. A grading system for RS has already been proven to add prognostic valuable information, independent of other factors like Gleason score (GS) and Prostate specific antigen (PSA), to today's predictive model. Altered metabolite concentrations have been found in PCa tissue *versus* normal tissue, and in high grade *versus* low grade PCa regarding citrate, spermine and choline containing compounds. The purpose of the study was to investigate whether there is a correlation between RS grade (RSG) and metabolite concentrations. The hypothesis is that RS is an active tissue that is important for cancer development and progression. Because some RSGs have been proven to lead to a worse prognosis than others, one would expect to find an alteration in phenotypes and metabolite concentrations between the different grades. Thereby this could lead to a better understanding of the molecular mechanisms in RS.

Methods

The tissue samples in the study came from 48 patients who underwent prostatectomy at St. Olavs Hospital, Norway. A new harvesting method was used to obtain one transversal fresh frozen slice from each of the prostates. Later, several samples from each slice were chosen for further examination. Metabolic spectra were acquired by High resolution magic angle spinning (HR-MAS) magnetic resonance spectroscopy (MRS) and each metabolite was quantified by LCMoDel. A histopathological evaluation considering RSG, GS and tissue composition was made on hematoxylin, erythrosine and saffron (HES) stained sections. The total number of samples was 149, of which 104 contained cancer. Finally, statistical analyses were performed in R to correlate RSG and metabolic concentrations. Linear mixed model (LMM) was used due this model's ability to adjust for intra-patient correlation, as there are several samples from each patient in our dataset. Fixed effects also adjusted for in the LMM were GS, percentage of tumor, stroma and luminal space. In addition, the Benjamini-Hochberg false discovery rate was applied to correct for multiple testing. Descriptive analyses and log-transformation of the metabolite concentrations were performed in SPSS.

Results

RSG was graded in the 104 samples that contained cancer tissue. In the dataset, 23 of the samples were graded as RSG 0, 59 graded RSG 1, 16 graded RSG 2 and 6 graded RSG 3. Initially LMM proved significant differences in the concentrations of citrate ($p=0,0071$), ethanolamine ($p= 0,0373$) and glucose ($p= 0,0100$) between different grades of RS. However, ethanolamine and glucose showed lack of standard deviation in qq-plots, and therefore the correlation could not be confirmed. After correction for multiple testing, the p-value for citrate concentration became non-significant ($p=0,1150$).

Discussion/conclusion

The results showed that citrate concentration significantly correlated with RSG before correction for multiple testing. Citrate has previously been shown to have a negative correlation with tumor aggressiveness and GS, but these factors were adjusted for in our model. Hence the RSG can be considered to be an independent predictor of citrate concentration. This strengthens the impression of epithelial-stromal interactions as an active contributor in cancer development and progression. However, because the results did not remain significant after correction for multiple testing, it is not possible to conclude anything. Whether a correction for multiple testing was necessary in this case, or if the correction may have lead ty a type II error, can be discussed. Regardless, the association between RSG and citrate concentration is interesting and needs further investigation. Both RSG and MRS have the potential of being implemented in routine diagnostics, and their significance has already been proven in other studies.

Preface

This medical student thesis has been carried out in the MR Cancer Group, Department of Circulation and Medical Imaging, Faculty of Medicine at Norwegian University of Science and Technology. Working with the thesis, we have obtained insight in challenges regarding prostate cancer, and possibilities that address solutions to these issues. Our focus has been on stromal-epithelial interactions and the metabolic alterations that occur in cancer development and progression.

We would like to thank our supervisor Dr. May-Britt Tessem for excellent guidance and support during the entire process. She is also responsible for acquiring the metabolic spectra used in this thesis. We also thank our co-supervisor Prof. Tone F. Bathen, head of the MR Cancer Group, as well as Alan J. Wright from Cancer Research UK, University of Cambridge, who performed the quantification of metabolic concentrations. We would in addition like to thank uropathologist Elin Richardsen at UIT, the Arctic University of Norway, for evaluating the histopathology. The statistical analyses we performed ourselves, however with invaluable help from research fellows Ailin Falkmo Hansen and Leslie E. Wood.

Hanna Stoll

Stud. med.

Hanne Schistad Robak

Stud. med.

Table of Contents

Abstract	III
Preface.....	V
Abbreviations	IX
1 Introduction	X
1.1 Prostate Cancer	1
1.1.1 The Prostate Gland	1
1.1.2 Features of Prostate Cancer	1
1.1.3 Epidemiology of Prostate Cancer	2
1.2 Diagnostics and Treatment of Prostate Cancer.....	3
1.2.1 Symptoms of Prostate Cancer	3
1.2.2 Digital Rectal Examination.....	3
1.2.3 Prostate Specific Antigen.....	4
1.2.4 Transrectal Ultrasound guided Biopsies.....	5
1.2.5 Histological Grading with Gleason Score.....	5
1.2.6 Clinical Staging with TNM.....	6
1.2.7 Risk Stratification.....	7
1.2.8 Treatment.....	7
1.2.9 Issues of Diagnostic and Treatment Strategies	8
1.3 Reactive Stroma.....	9
1.3.1 Reactive Stroma Definition.....	9
1.3.2 Reactive Stroma in Prostate Cancer	10
1.3.3 Histological Appearance.....	11
1.3.4 Predictive Value.....	12
1.4 Metabolomics	13
1.4.1 Metabolic Alterations in Cancer.....	13
1.4.2 Metabolic Alterations in Prostate Cancer	14
1.5 Magnetic Resonance Spectroscopy.....	17
1.5.1 Theoretical Basics of Magnetic Resonance Spectroscopy.....	17
1.5.2 <i>In vivo</i> Magnetic Resonance Spectroscopy	18
1.5.3 High Resolution Magic Angle Spinning.....	18
1.5.4 Magnetic Resonance Spectroscopy and Prostate Cancer	19
1.6 Absolute Quantification of Metabolites by LCModel	20
1.7 Statistics	21
1.7.1 Linear Mixed Model.....	21

1.7.2 The Benjamini-Hochberg False Discovery Rate	21
2 Purpose.....	23
3 Materials and Methods	25
3.1 Overview of Methods.....	25
3.2 Patient and Tumor Characteristics	26
3.3 Harvesting Method.....	26
3.4 Selection of HR-MAS Samples	27
3.5 HR-MAS Experiments	28
3.6 Quantification of Spectra by LCMModel	28
3.7 Grading of Reactive Stroma	28
3.8 Statistical Methods.....	29
3.8.1 Descriptive Statistics.....	29
3.8.2 Linear Mixed Model.....	30
4 Results.....	33
4.1 Histopathology.....	33
4.2 Overview of quantified Metabolites	35
4.3 Metabolic Changes between different Reactive Stroma Grades.....	36
4.4 Metabolic Changes Regarding Reactive Stroma Grade with LMM.....	38
4.4.1 Adjusted Models for Ethanolamine and Glucose.....	39
4.4.2 Adjusted Model for Citrate.....	39
4.4.3 Adjusting for Luminal Space	40
4.4.4 Metabolic Changes regarding RSG when considering all Samples.....	40
4.5 Summary of Citrate Changes	41
5 Discussion	43
5.1 Reactive Stroma and Metabolomics	43
5.2 Importance of Different Reactive Stroma Grading Systems	43
5.3 Metabolite Changes in Reactive Stroma.....	45
5.3.1 Citrate	45
5.3.2 Spermine	46
5.3.3 Choline and Choline Containing Compounds	46
5.4 Correction for Multiple Testing	47
5.5 Strengths and Limitations	49
5.6 Clinical Translation	50
6 Conclusion	53
7 Appendix.....	55
8 References.....	59

Abbreviations

ACON	m-aconitase
BH	Benjamini Hochberg
BPH	Benign prostate hyperplasia
CAF	Cancer associated fibroblasts
CC/C	(Choline + creatine)/citrate
CCP/C	(Choline + creatine + polyamines)/ citrate
Cho	Choline
ChoCC	Choline containing compounds
cT	Clinical tumor stage
DRE	Digital rectal examination
ECM	Extra cellular matrix
EGF	Epidermal growth factor
FDR	False discovery rate
GPCho	Glycerophosphocholine
GS	Gleason score
HES	Hematoxylin Erythrosine Saffron
HR-MAS	High resolution magic angle spinning
LCModel	Linear combination of model spectra
LMM	Linear mixed model
LS	Luminal space
LUTS	Lower urinary tract symptoms
MAS	Magic Angle spinning
MR	Magnetic resonance
MRI	Magnetic resonance imaging
MRS	Magnetic resonance spectroscopy
MRSI	Magnetic resonance spectroscopy imaging
PCa	Prostate cancer
PCho	Phosphocholine
ppm	Parts per million
PSA	Prostate specific antigen
RS	Reactive stroma
RSG	Reactive stroma grade
s-ALP	Serum alkaline phosphatase
s-PSA	Serum prostate specific antigen.
TCA	Tricarboxylic acid
tCho	Total Choline
TGF-α	Tumor growth factor α
TNM	Tumor, nodes, metastasis
TRUS	Transrectal ultrasonography
TUR-P	Transurethral resection of the prostate

1 Introduction

1.1 Prostate Cancer

1.1.1 The Prostate Gland

The prostate is a glandular, chestnut-sized structure situated between the bladder and the pelvic floor, surrounding the first part of the male urethra (figure 1.1). It is positioned ventrally to the rectum, only separated by a thin layer of connective tissue. This makes it available for palpation by digital rectal examination (DRE) [1]. The prostatic gland is enveloped by a capsule of dense connective tissue, and can be separated into three zones (figure 1.2). The transition zone is the smallest and surrounds the upper third of the urethra, whilst the central zone makes up the center of the prostate where the two ejaculatory ducts enter into the urethra. The peripheral zone represents the main part of the prostate tissue [2].

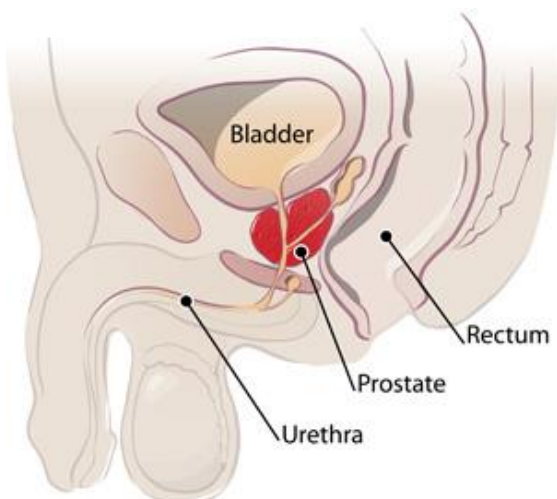


Figure 1.1: Location of the prostate [3].

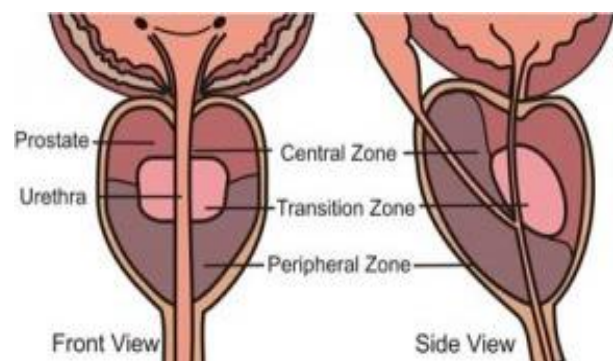


Figure 1.2: The three anatomical zones of the prostate [4].

The main function of the prostate is the production of an alkaline, thin fluid, which is secreted into the urethra during ejaculation. This makes up 30% of the ejaculation volume. The secretion neutralizes the low pH of the vaginal environment, thereby enhancing sperm motility and survival [1].

1.1.2 Features of Prostate Cancer

Adenocarcinomas, originating from the acini and ducts of the prostate, make up 95% of prostate cancers (PCa). The majority of adenocarcinomas derive from the peripheral zone. Many of these tumors grow multifocal within the prostate, and therefore they are not necessarily palpable during DRE [5]. The adenocarcinoma group can be subdivided further into an acinar type, which makes up the

vast majority, and is often referred to simply as prostate carcinoma. Other subgroups constitutes less than one percent of adenocarcinomas, and have a much poorer prognosis. This group includes ductal, signet ring, mucinar and small-celled adenocarcinomas [5]. PCa derived from other tissue types, such as urothelial carcinomas, sarcomas and lymphomas, makes up the remaining 5% of PCa. Metastasis to the prostate can occur, but is very rare. It is by far more usual for cancerous tumors in neighboring organs (bladder, rectum, testicles) to grow directly into the prostatic gland [5].

In the beginning of the cancer development, PCa grows locally inside the gland. It can do so for many years before it infiltrates through the fibrous capsule into the connective tissue surrounding the prostate. Then the cancer can grow into neighboring structures, such as the seminal vesicle, the urethra and the bladder. Metastasis can occur at any cancer stage, both lymphatic and haematogenous. Metastases are most frequently found as osteosclerotic lesions affecting the red bone marrow of the spine, pelvis, ribs and skull [6].

1.1.3 Epidemiology of Prostate Cancer

PCa is the most frequent type of cancer found in men in Norway and most of the western world. Worldwide it is the 4th most common cancer diagnosis, with 1.1 million estimated cases in 2012 [7]. In Norway, between 2005-2009, on average 4100 new cases were diagnosed each year, which makes up 30% of the total incidence of male cancer. It is estimated that one in eight men will be diagnosed with PCa before turning 75 years of age [8, p. 16, 9]. Even though PCa occurs among 17% of Norwegian men, only 3-4% die because of their diagnosis [9].

There are no known causes of PCa. The most important risk factors identified are high age (highest diagnose rate between 70-80 years of age [10]), family accumulation and race [8, p. 30]. Several other risk factors have been suggested, such as diet, physical activity and smoking. However, to this date, no certain relations have been detected [8, p. 24]. There are tremendous variances in PCa incidence rates found in different ethnical groups and countries, with the lowest incidence rate in Asia and the highest in the Afro-American population in the U.S.A. This can be explained partly by environmental differences, varying usage of diagnostic tools and different levels of health care in general. But this ethnical difference in incidence also strengthens the theory of genetic factors as a contribution to PCa development [8, p.16].

Because of the growing usage of Prostate specific antigen (PSA) measurements as well as increasing life expectancy, a great surge in PCa incidence is seen in Norway and other developed countries. In Norway, the incidence rate has been as much as doubled during the last 25 years [8, p. 16]. Even though the incidence of PCa in Norway is increasing, the mortality of the disease has been stable and even slightly decreasing. This means that more men are diagnosed with PCa and living with their disease. Because of this increased prevalence, there is a huge demand for a precise and effective follow-up system [8, p. 16].

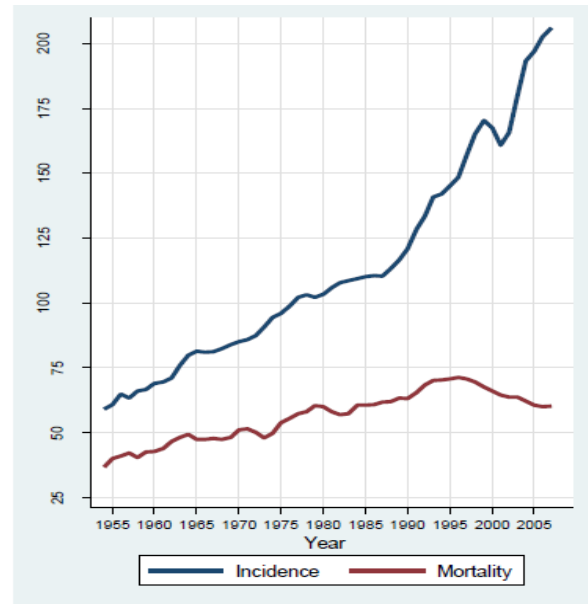


Figure 1.3: Age-standardized incidence and mortality rate of PCa in Norway. [8,11]

1.2 Diagnostics and Treatment of Prostate Cancer

1.2.1 Symptoms of Prostate Cancer

In early stages of PCa there are rarely any symptoms. If the cancer grows to become locally advanced, lower urinary tract symptoms (LUTS) can occur. However, these symptoms are more likely to be the result of benign prostate hyperplasia (BPH) or other benign conditions. Still, the possibility of PCa ought always to be considered in a patient presenting LUTS [8, p. 33, 12]. In metastatic disease, bone pain, fatigue, anemia, and weight loss can be present [12].

Current methods to diagnose PCa include a clinical examination with DRE, PSA serum measurements, Magnetic Resonance Imaging (MRI) and transrectal ultrasound (TRUS) with biopsies. In addition, high-risk patients are examined with scintigraphy and other imaging modalities. A suspicious DRE and/or elevated PSA indicates further investigation with imaging and biopsies. The results of the histology, staging and PSA-testing, stratify the patients into risk groups that determine their course of treatment.

1.2.2 Digital Rectal Examination

Because 75% of PCa is located in the peripheral zone of the prostate, sometimes nodules, asymmetry and enlargement can be palpated by DRE. However, PCa is often multifocal and without palpable

nodes, so in many cases DRE gives a false negative result. If the DRE presents suspicious findings, biopsies are indicated, regardless of serum PSA (s-PSA) measurements [12].

1.2.3 Prostate Specific Antigen

PSA is an enzyme, a protease that is exclusively produced by the epithelial cells of the prostate. It is a glycoprotein that can be measured in the serum. The function of the protein is to prevent the seminal fluid from coagulating. It is prostate specific, but not PCa specific. Other conditions that can give rise to elevated PSA levels are BPH, prostatitis and lower urinary infection. [8, p. 33, 13]. The higher the s-PSA level, the more likely malignancy is the cause of the increase. The reference value increases with age, but there is no absolute cut-off (table 1.1). However, s-PSA of 3-4 µg/L in more than two repeated measurements is often considered as suspicious or pathological [12].

In screening, s-PSA has a sensitivity of only 21% and a specificity of 91%, when the reference value is set at 4 µg/L [14]. Hence, there is a large amount of patients with PCa which the test is not able to detect. At the same time, 10% of healthy men get a false positive result, followed by excessive diagnostics and overtreatment. [12] The rate of s-PSA increase between two measurements (PSA-velocity) is also an important variable to consider.

Age	s-PSA level
0-49	0-2.5 µg/L
50-59	0-3.5 µg/L
60-69	0-4.5 µg/L
>69	0-6.5 µg/L

Norwegian health government does not recommend PSA screening in the general population. PSA screening programs have not been proven to increase total survival, though they have been discovered to reduce the risk of death due to PCa [8, p. 26-31]. There have been two major studies (ERSPC and PLCO) on the subject, but none of them have been able to prove the benefit of PSA screening opposed to the negative effects of immense overtreatment [16]. Hence, the Norwegian Directory of Health only recommends PSA screening in patients with familial accumulation of PCa [8, p. 26-31]. Nevertheless, when there is a clinical suspicion of PCa, such as LUTS or positive DRE, PSA testing is recommended, as it is testing with a diagnostic purpose and not screening of an assumed healthy person.

1.2.4 Transrectal Ultrasound guided Biopsies

Biopsies are indicated if s-PSA >3-4 µg/L in more than two repeated measurements or if the DRE is suspicious. In patients with a life expectancy below ten years and no symptoms, however, it should be considered to refrain from further examinations. [8, p. 37]. Primarily, at least ten biopsy specimens should be obtained with ultrasound guidance, five from each lateral lobe. Further biopsies might be indicated later on. Usually MRI is performed before the TRUS-guided biopsies, as the biopsy procedure can lead to small hemorrhages that can affect the image quality. Side effects of the biopsy procedure are pain, infection or bleeding. Due to the increasing antibiotic resistance, infections follow as a growing problem [12]. Tissue samples can also be collected from transurethral prostate resection (TUR-P) or radical prostatectomy.

1.2.5 Histological Grading with Gleason Score

Histological grading is essential to set the PCa diagnosis. The main system for histological grading is the Gleason grading system, which grades the architectural appearance and atypia of the tumor tissue from one to five. It is one of the most important prognostic factors for PCa [5].

In Gleason grade 1 the glands resemble normal prostate tissue, while in grade 4 and 5, normal gland architecture is lost. In high grade cancers, the tumor is poorly differentiated, grows in sheets, and the stroma is evaded or could be absent [5, 8, p. 39]. Finally, a Gleason score (GS) is obtained by summarizing the most dominant grade and the second most dominating grade in the biopsy. The second most dominant grade is considered only if it makes up more than five percent of the biopsy. Grade 4 and 5 are exceptions from this rule and are always incorporated into the GS, regardless of amount. Hence, the maximum GS is ten, which indicates an aggressive tumor and a bad prognosis [5]. Other elements in the biopsies that are considered are the number of cores containing cancer, tumor volume and perineural invasion [17, 18].

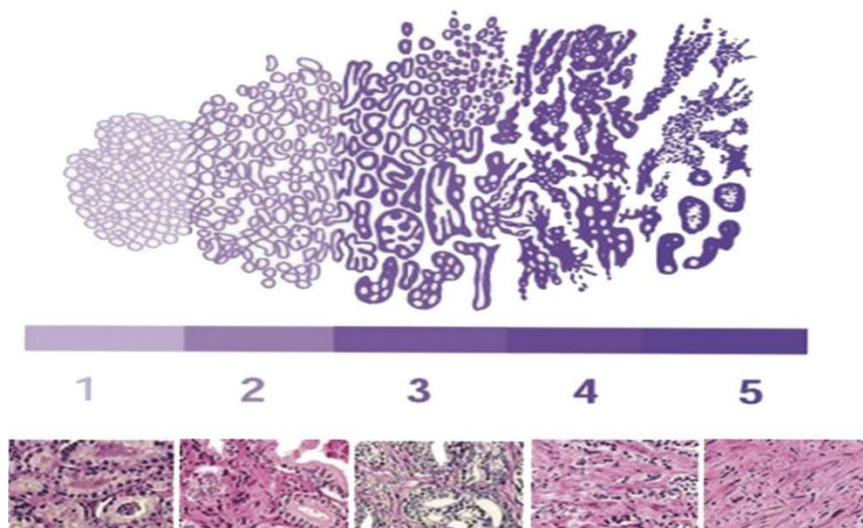


Figure 1.4: Histological appearance of the different Gleason grades [19].

1.2.6 Clinical Staging with TNM

The TNM system includes the tumors size, growth pattern and spread at the time of diagnosis (table 1.2). These parameters provide information about cancer aggressiveness and growth rate. Hence, the staging is an important prognostic factor. PCa can be local, locally advanced or metastasized. The size, local growth and invasiveness is graded T1-T4. An important distinction is between intra capsular (T1-T2) and extra capsular (T3-T4) PCa, because it affects the course of treatment. DRE and MRI are used to determine the T-stage. In addition, TRUS and biopsies can be helpful. Whether the tumor has spread to regional lymph nodes (N1) might be important for the intention and choice of treatment. A high PSA level, T-stage or GS indicates a high risk of lymph node metastases. The gold standard to detect whether lymph nodes are affected, is surgical lymphadenectomy. Nevertheless, lymphadenectomy should be executed only if the information it provides influences the choice of treatment. MRI can be a useful modality for determining the N-stage as well [8, p. 44-46, 13, 21, s. 28]. Cases with intermediate- or high risk of distant metastases (M1) are examined with scintigraphy and MRI. PSA is a good measurement to stratify these patients. The skeleton is the most prevalent place for metastases, and serum Alkaline Phosphatase (s-ALP) can therefore be used as an indicator for metastases in addition to PSA. If the intention of treatment is curative, a scintigraphy is usually performed regardless of metastatic risk [8, p. 47].

Table 1.2: TNM system of PCa		
T: Local growth and invasion of the primary tumor	T1	Not detectable by palpation or imaging. Diagnosis is made by biopsies.
	T2	Palpable or visible, but limited to the prostatic gland.
	T3	Growth through the capsule of the prostate and/or into the seminal vesicle.
	T4	Infiltrates neighbouring organs.
N: Invasion of local lymph nodes.	N0	No invasion detected.
	N1	Invasion detected.
M: Distant metastases	M0	No metastases detected.
	M1	Metastases detected.
Table content is modulated from oncolex [20].		

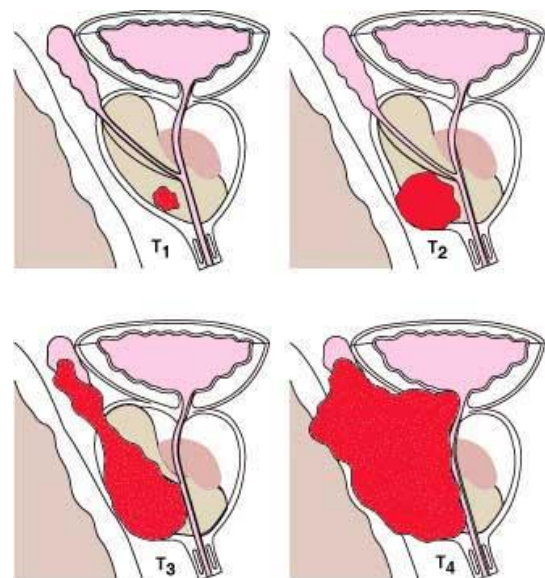


Figure 1.5: T-stage of PCa. From pathology outlines [22]

1.2.7 Risk Stratification

To choose the intention and course of treatment, it is crucial to evaluate the different prognostic factors together. Today the most important factors are PSA, clinical T-stage and GS. Whether the disease is local, locally advanced or metastasized, decides if the treatment intention is curative or palliative. In addition, the number of positive biopsies, patient age, fitness and motivation are considered. There are no distinct cut-offs and therefore each case must be evaluated separately [8, p.49].

Risk group	Clinical T-stage		PSA (ng/ml)		Gleason score
Low	T1c-2a	and	<10	and	≤6
Intermediate	T2b-c	or	10-20	or	7
High	≥T3	or	>20	or	≥8

Table is modulated from Norwegian Guidelines for PCa [8, p.49].

1.2.8 Treatment

Because PCa is such a heterogeneous cancer, diagnostics and choice of treatment are challenging. The risk stratification can help to make a decision, but it is not capable of separating between aggressive and indolent cancer in a sufficient way, especially in the early stages of cancer development [23]. Choice of treatment also depends on the autonomy of the patient.

With a curative intention, either active surveillance or active treatment are possible options. The surveillance aims to prevent overtreatment, but at the same time detect cancer progression so treatment can be started immediately if necessary. The patient is monitored closely with PSA measurements and biopsies, and should be in the low risk category to follow this program [8, p. 51, 12]. There are several choices and combinations of active treatment. Radical prostatectomy is the gold standard for T1 and T2 cancers if the patient has more than ten years estimated life expectancy [12]. With locally advanced cancer, surgery is still possible in some cases, but is usually more extensive. In addition, adjuvant radiation and/or hormonal therapy is necessary. Primary radical radiation is also an option for locally advanced or aggressive cancer. New methods with internal cryotherapy or brachytherapy can also be used adjuvant to external radiation [8, p. 52-54, 12].

Palliative treatment is intended for patients with metastatic or locally advanced cancers, or old and weak patients with a short life expectancy. The treatment focuses on symptom relieve and life quality.

Therefore, a lower amount of side effects is accepted than in curative treatment. Hormonal therapy is the corner stone in the palliative treatment [8, p. 83-85, 24]. It works by inhibiting the effects of androgens, which function as growth factors on the prostate, and therefore also the PCa. Hormonal therapy acts on different levels, either by inhibiting the secretion of androgens from the testicles, by surgical or medical castration, or by inhibiting or blocking the effect of circulating peripheral hormones. Often these targets are used in a combination. Surgery, radiation or chemotherapy might be indicated as well to relieve pain and symptoms from the urinary tract and metastases [8, p. 83-85, 21, p. 56, 24]. Surgery, radiation and hormonal therapy all have side effects that have to be evaluated up against the benefit of treatment. This is a major issue in today's management of PCa.

1.2.9 Issues of Diagnostic and Treatment Strategies

Some cases of PCa are extremely aggressive and dangerous, but most cases are silent and slow growing. The indolent cases will possibly never give symptoms during the patient's life span. The diagnostic methods we have today are not capable of predicting the clinical behaviour of the tumor in a sufficient way [23, 25]. Therefore, the course of treatment in each individual patient is often uncertain. This leads to both under- and over-treatment.

PSA is challenging in the sense that it lacks both specificity and sensitivity, and it is a huge discussion whether PSA should be screened or not. Medium high PSA-levels can be caused by benign conditions, which will give false positive results [26]. It is estimated that 70-80% of men over 60 years of age have a histological BPH, and therefore elevated PSA levels are extremely common in the older male population. These elevated, benign PSA levels will in many cases be followed by further diagnostics and biopsies [27]. If 4 µg/L is used as threshold for PSA levels, the sensitivity is 21% [14]. That means that 79% of men with PCa have a value below the threshold, and their disease will go undetected unless they have a suspicious DRE. The specificity is 91%, which in turn means that almost 10% of men without cancer will have false positive tests [14]. If all men in the population are tested, these 10% make up a huge amount of potential patients. Hence, both the negative and positive predictive value of the test is poor. On the positive side, PSA screening makes it possible to detect cancer earlier and therefore stop potentially aggressive PCa before it has spread. However, when cancer is detected in a silent and localized stage it is difficult to know whether it ever will be clinically significant. The screening-detected cancer might not give any symptoms during the patient's lifespan, but demands a lot of resources from the health care system and provides worries and inconvenience

for the patient. Treating indolent cancer can possibly cause side effects and complications that reduce the patient's quality of life [8, p. 29, 28, 29].

Another problem with PCa diagnostics is the sensibility of biopsies. Because the cancer has a multifocal growth, it is easy to miss representative tissue when taking samples and therefore underestimate the cancer during the histological evaluation. MRI and TRUS-guided biopsies increases the success rate, while traditional biopsy methods without guidance may miss up to 50% of tumor foci [17, 25]. In addition, the GS is not capable to accurately estimate tumor aggressiveness and rate of progression as it only considers the architecture of the epithelial glands. Especially low and intermediate graded tumors are difficult to predict. Hence, the risk stratification and subsequent choice of treatment could be wrong [25].

Finally, treatment is always followed by side effects. Patients with indolent cancer that are receiving treatment like surgery, radiation or androgen deprivation, are in danger of complications like erectile dysfunction, urinary incontinence and bowel problems. The ERSP study on PSA screening has estimated that the number needed to screen is 1410, while the number needed to treat is 48 to prevent one death due to PCa [8, s. 25]. That means that in a worst-case scenario, 47 prostates have to be removed with the following complications for each live saved.

1.3 Reactive Stroma

1.3.1 Reactive Stroma Definition

Desmoplasia, or reactive stroma (RS), is a histological interaction that occurs between a tumor and the native host connective tissue [18]. It is defined as a change in stromal composition, evoked by a carcinogenic process or as a reaction to injury [17]. In various studies it has been proven that the desmoplastic response seen in different human cancers, such as breast, cervix, colon and lung, plays a key role in tumor spread and progression. It is believed that tumorous epithelial cells in reciprocal interaction with stromal cells and various molecules of extracellular matrix (ECM), create a microenvironment suitable for cancer cell proliferation, movement, and differentiation. These interactions are carried out by various signalling pathways, growth factors, etc. As an example, the stroma can inhibit infiltration of immune cells into the tumor area, thereby protecting it from host defense [17, 30].

1.3.2 Reactive Stroma in Prostate Cancer

In an undisturbed environment, normal prostate stroma contains smooth muscle cells, which under the influence of androgens, signal to the prostatic epithelium to maintain differentiation and repress proliferation. The prostatic epithelium in turn signals to prostatic smooth muscle cells to maintain their differentiated phenotype [17]. The RS in PCa is characterized by a fundamental alteration in stromal cell phenotype and composition of ECM. Instead of smooth muscle, the prostatic stroma changes to contain increasing numbers of myofibroblasts, also called Cancer associated fibroblasts (CAFs). This new cell phenotype is responsible for ECM remodeling as well as an increase in local vascular density. The myofibroblasts have been proven to secrete growth factors, such as Epidermal growth factor (EGF) and Transforming growth factor- α (TGF- α), which stimulate the cancerous epithelial cells [30, 31]. It is important to note that RS in the prostate is not exclusive to cancer, but can also be observed in acute or chronic prostatitis and atrophic processes [17].

PCa-associated RS is composed of a myofibroblast/fibroblast mix with a significant decrease or complete loss of fully differentiated smooth muscle cells [32]. RS myofibroblasts are coexpressing markers of both smooth muscle cells and fibroblasts. At the same time, some late stage markers of smooth muscle differentiation are lost [31]. This knowledge can be used to create immunohistochemical stains to identify areas of RS (figure 1.6) [17]. However, as described by Yanagisawa et al., RS identification and grading is possible also on Hematoxylin Erythrosine Saffron (HES) stained biopsy samples [17].

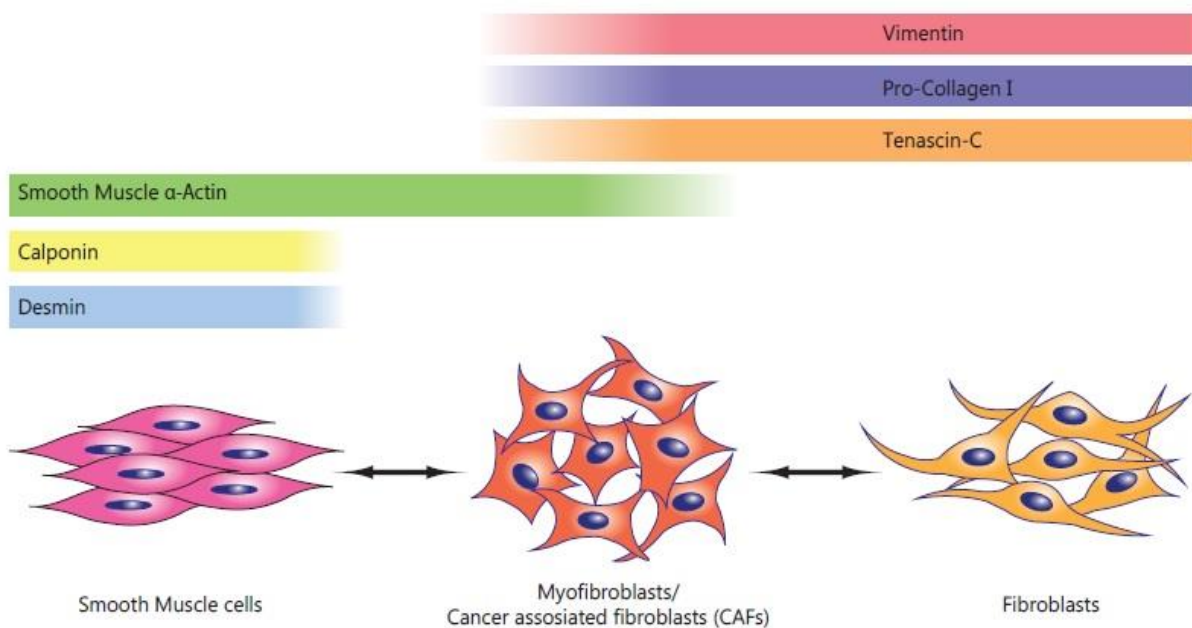


Figure 1.6: Major cell phenotypes of PCa stroma and associated marker proteins. The figure is modulated from Barron et al. [31] and includes information from Yanagisawa et al. and Ayala et al. [17, 18].

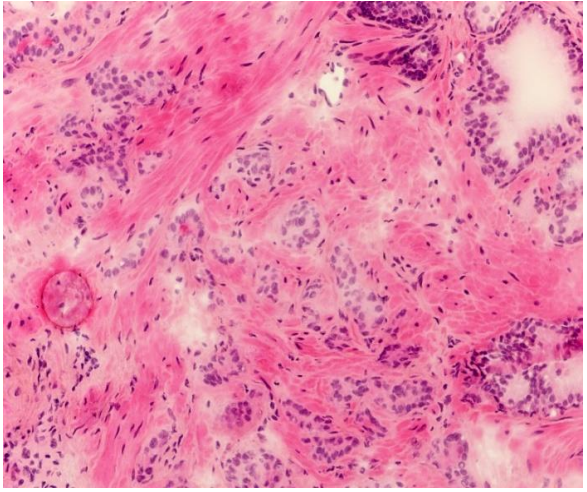
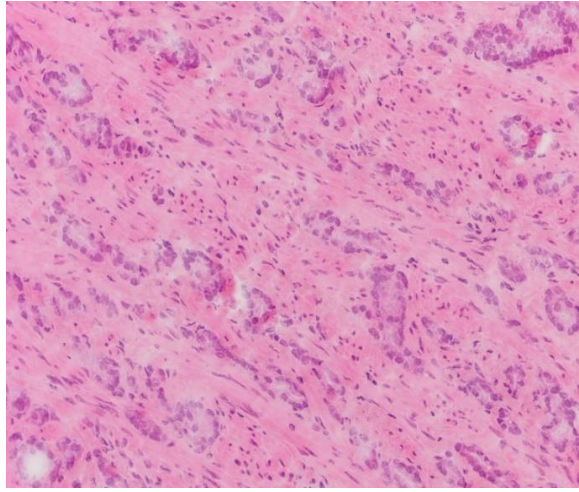
1.3.3 Histological Appearance

In most organs, such as breast, colon and lung, the desmoplastic response to cancerous processes present itself as fibroblast acquiring myofibroblastic features. These changes can easily be spotted during routine histological diagnostics on HES-stained probes. However, RS is more difficult to detect in the prostate, because the change from smooth muscle to myofibroblast does not change the histological appearance in the same manner. Hence, the stromal response is often described as “masked” [17].

In healthy prostate tissue, the smooth muscle cells are organized in bundles. The cells are uniform and contain abundant and dense eosinophilic cytoplasm as well as rounded nuclei [17]. In reactive stroma the cells look paler, have elongated nuclei and less cytoplasm. They appear more fibroblastic than normal smooth muscle, running in disorderly patterns with irregular length and thickness [17]. There is deposition of collagen fibrils and ECM, forming an irregular, loose and fibrillary background pattern [17].

It is possible to grade the RS with a standardized method that has been described in previous studies [17, 32]. This method uses a scoring system that separates RS into grades based on the ratio between RS and cancer epithelium: Grade 0, none or up to 5% RS; grade 1; 6%-15% RS; grade 2, 16%-50% RS; grade 3, 51%-100% RS. Grade 3 demands a ratio between stroma and cancer epithelium of more than 1:1. In reactive stroma grade (RSG) 3 there is more reactive stroma than epithelial cells, and is therefore referred to as stromogenic cancer. This gives the tissue a distinct appearance. The epithelial glands appear sharp-edged, angulated and pinched, while the lumen of the glands is squeezed or collapsed [17]. RSG 0 can be seen in both cancer with high GS, where there is a general lack of stroma, and cancer with abundant stroma, but where a desmoplastic response is lacking [33].

Table 1.4: Comparison of RSG 0 and RSG 3

(A) RSG 0	(B) RSG 3
	
<p>Both of the pictures above have a low grade GS ($\leq 7a$), but there is a distinct difference in stromal composition. (A) RSG 0. 0-5% reactive stroma. The ECM consist of bundles of pink smooth muscle cells. The cytoplasm has a dense eosinophilic color. (B) RSG 3. There is an obvious desmoplastic response. The ECM has a paler and more fibrillary appearance, and there is a lack of smooth muscle cells.</p>	

1.3.4 Predictive Value

As the RS plays an important role in the development of PCa, the grading and quantification can serve as a marker for PCa aggressiveness. In the latter years, quite a few studies have revealed new information about the significance of RS. In 2003 a pioneer study by Ayala et al. [32], demonstrated that non-epithelial RS elements in PCa could be used as a prognostic indicator. By grading the amount of RS in radical prostatectomies, it was discovered that patients with RSG 0 and RSG 3 had significantly lower biochemical recurrence-free survival rates compared to patients with RSG 1 and 2 [32]. Studies by the same research group later showed similar findings in needle biopsies. It was stated that the grading of RS can function as an independent predictor of PCa recurrence opposed to PSA and GS [17]. Of special interest is stromogenic cancer (RSG 3), which could be observed in all Gleason grades. In 2011, Ayala et al. [18] published that the quantification of stromogenic cancer in prostatectomy specimens was significantly predictive of PCa-specific death, with higher quantities of RSG 3 leading to decreased biochemical recurrence-free survival.

In addition, more recent studies have shown a correlation between RSG and PCa survival [33, 34]. However, the correlation was more linear, with the risk of PCa-specific mortality rises as the RSG increased [33]. Hence, RSG 0 was associated with the highest survival rates, opposing previous findings by Alaya et al. In their study, Sæter et al. proved that adding RSG to the current predictive model,

consisting of PSA-level, GS and clinical T-stage, increased the power of the model [33]. In addition, Billis et al. [34] could report significant association of increasing RSG with several clinicopathological findings, such as high T-stage, preoperative PSA and GS. They found RSG 3 to be a negative predictive factor of biochemical recurrence free survival, but were not able to prove this finding to be independent of other clinicopathological predictors.

Even though there are discrepancies in the significance of RSG, it is safe to say that RS and its grading holds information on cancer aggressiveness and recurrence risk that does not overlap with current predictive tools. RS in general, but especially RSG 3, demonstrates biomarker potential for the diagnostics, risk stratification and follow up of PCa. However, further studies are needed before the grading and quantification of RS can be incorporated into routine PCa diagnostics [17, 18, 33].

1.4 Metabolomics

1.4.1 Metabolic Alterations in Cancer

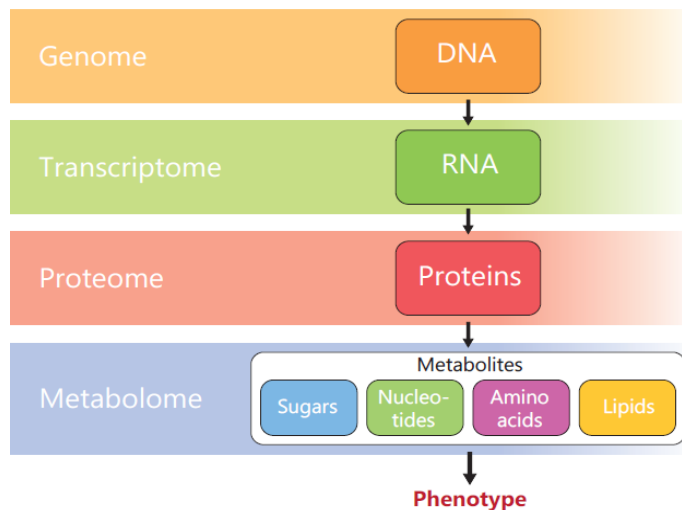


Figure 1.7: Flow of information from DNA to phenotype [36].

Each cell in the body is producing a distinct set of metabolites. The type and amount of metabolites are expressed as the cell's phenotype, and is the product of genes, gene expression, protein production and metabolism (figure 1.7) [35]. Identification and quantification of these metabolites provides information about processes within the cell, which is the center of the emerging field of metabolomics.

Cancer changes gene expression and further modifies the rate of cell growth, survival and function. The hallmarks of cancer are a set of properties that together lead to uncontrolled growth, invasion and metastasis (figure 1.8) [37, p. 161, 38, 39]. Alterations in the cancer cells result in a different metabolic profile, with distinct changes in metabolite concentrations. These concentrations can be measured and used as biomarkers, which can provide valuable diagnostic and prognostic information [23, 40, 41].

1.4.2 Metabolic Alterations in Prostate Cancer

In PCa cells, several metabolic changes have been detected, and recent studies have shown that metabolic profiles may reflect the cancers aggressiveness and its potential to progress and metastasize [25, 40-42]. Tumor cells divide and proliferate, and a consequence of this is an altered energy demand and an increase in lipid biosynthesis, especially for cell membrane production. Because of these requirements, the metabolism of the cancer cell changes, giving rise to altered metabolite concentrations [38, 43].

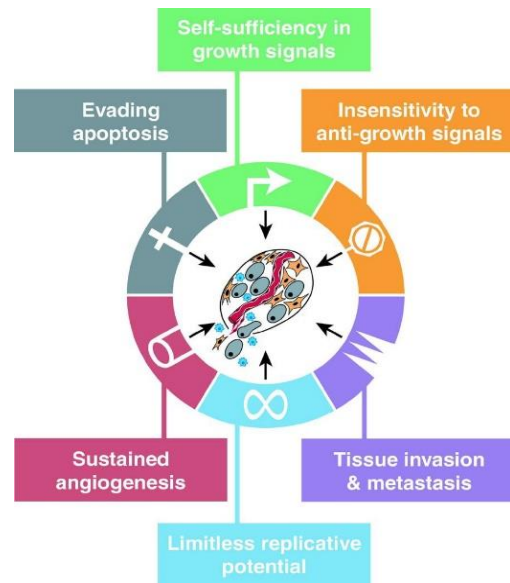


Figure 1.8: The hallmarks of cancer. The picture is obtained from Hanahan et al [39].

Citrate

Benign prostate tissue contains high levels of citrate, an intermediate in the tricarboxylic acid (TCA) cycle [42]. Decreased citrate levels have been linked to progression of PCa [23, 35]. In a healthy prostate cell, citrate is produced in large amounts in the mitochondria. This is because the enzyme m-aconitase (ACON), responsible for the oxidation of citrate to iso-citrate, is inhibited by zinc and therefore limits the TCA cycle, leading to an accumulation of citrate. Citrate is transported to the cytosol and secreted into the spermatic fluid in the luminal ducts, where it serves as an energy supply for the sperm cells. Citrate can also be used for the production of fatty acids and cholesterol in the cell cytosol (figure 1.9) [23, 38, 40, 43, 44].

In cancer cells, zinc transporters are downregulated and the ability to accumulate zinc inside the cell is lost. [38, 43, 45, 46]. Thereby the inhibition of ACON is lost, leading to increased oxidation of citrate in the TCA cycle for energy production. In addition, citrate is used as a metabolite in lipogenesis in the cytosol, because of an increased need for plasma membranes in dividing cells. As a result, less citrate is secreted into the luminal ducts [40, 46]. In addition, PCa cells have an uptake of citrate from the extracellular space instead of secreting it out of the cell [44]. The net effect of all these alterations is a lower level of measured citrate in PCa tissue. A 20-fold decrease of citrate concentrations in malign prostate glands can be observed. This decrease has the potential to be used as a diagnostics tool. Changes in citrate metabolism have even been shown to precede detectable pathological findings [44]. Citrate concentrations can also separate between high (GS ≥ 7) and low grade (GS=6) PCa, since the concentration correlates to aggressiveness and GS [23].

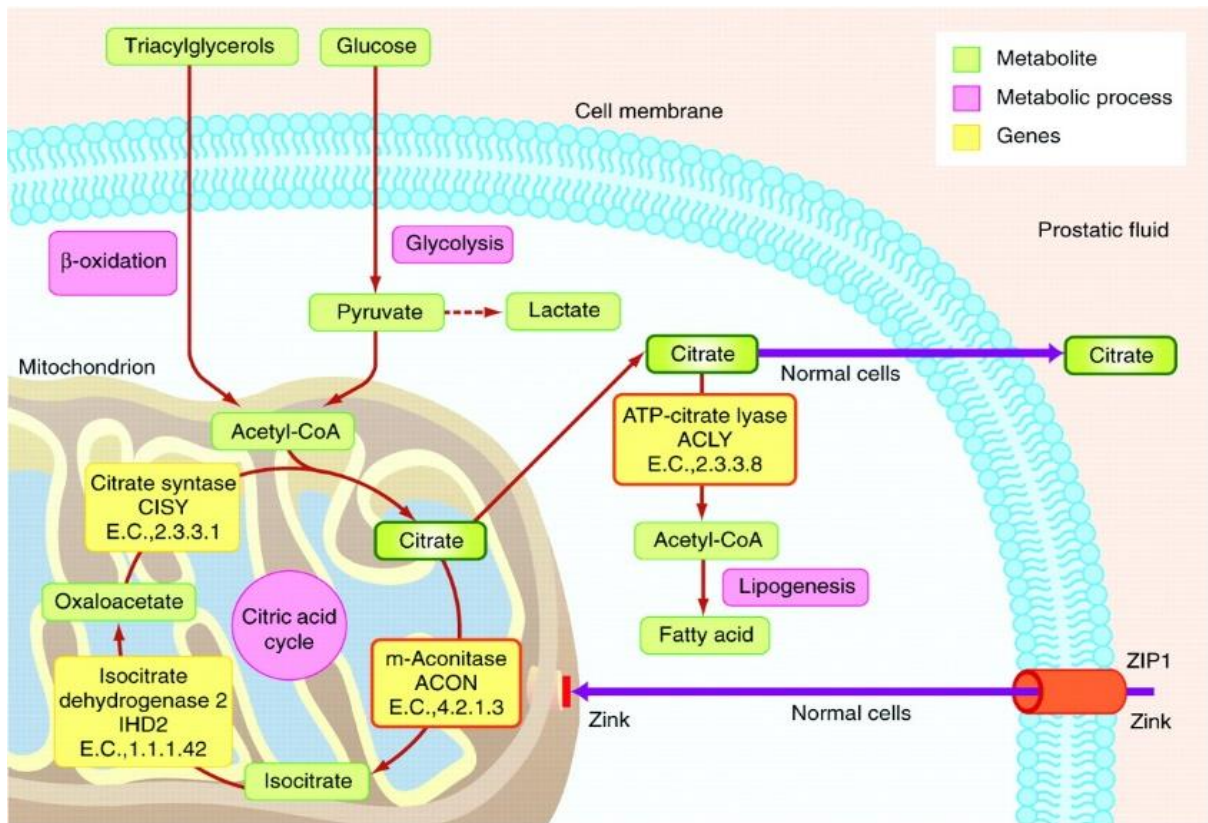


Figure 1.9: Citrate metabolism in a prostate cell. From Bertilsson et al. [40].

Lactate

When cancer cells proliferate, aerobic glycolysis increases dramatically. Aerobic glycolysis means that pyruvate is metabolized to lactate even if oxygen is available, instead of entering the TCA cycle. As the TCA cycle is downregulated, more citrate is available for lipid and membrane production. This is also known as the “Warburg effect”, and is a less effective way of producing energy than the normal TCA-oxidative phosphorylation pathway [43, 44, 47]. Hence, the demand for glucose in the cell is increased [47]. The aerobic glycolysis leads to an increased level of lactate, which later can be converted back to pyruvate and re-enter the citrate production [38]. In addition, cancer cells that proliferate faster than their blood supply, will experience hypoxia which leads to anaerobic glycolysis and further increasing lactate levels. There has been shown a highly significant increase in lactate in PCa cells compared to benign tissue [42].

Choline and Choline Containing Compounds

Choline is a nutrient that is used in phospholipid metabolism, cell membrane synthesis, acetylcholine production and as a methyl donor. Hence, it supports the cell proliferation that is necessary in cancer development [48]. Altered choline-phospholipid metabolism is a “new metabolic hallmark of cancer”,

that has emerged after the start of magnetic resonance spectroscopy (MRS) studies on tumors. A high level of choline in tissue has been related to an increased risk of cancer, and has shown potential as a metabolic biomarker [48]. Choline metabolism is activated in cancer cells and followed by an increase in Choline containing compounds (ChoCC), like phosphocholine (PCho) and glycerophosphocholine (GPCho) [49]. The increase in choline cannot be explained by the high rate of cell division by itself, but as the result of a “malign transformation” in the cancer cell. Benign cells that proliferate with the same rate as cancer cells, still do not reach the same levels of choline. An altered expression of enzymes and transporters involved in the pathway of choline is a part of the malign transformation, and is thought to be due to genetic and/or epigenetic changes [48, 49]. Molecules in the choline pathway can also function as second messengers in oncogene signaling [48]. Aggressive and high grade PCa (Gleason grade 4) has been shown to have higher levels of choline than low grade PCa in some studies [48, 50]. The concentration of ChoCC also correlates to the stage of PCa [48]. Nevertheless, other studies have not been able to prove the same correlation between choline and PCa aggressiveness [23].

Spermine

Spermine is a polyamine, together with putrescine and spermidine, which is present in all eukaryote cells and is an important molecule in many cellular mechanisms. Polyamines contributes in the regulation of cell proliferation and differentiation, and have been found to have an inhibiting effect on PCa [51, 52]. Altered levels of spermine and other polyamines have a strong association with cancer [53]. Therefore, spermine has been suggested as a marker for the normal secretory state of functional epithelial prostate cells [54]. Also, the level of spermine significantly decreases in high grade (GS \geq 7) compared to low grade (GS=6) PCa [23]. Polyamines have been shown to play an important role in detecting and stratifying PCa, and are therefore implemented into the MRS evaluation of the cancer [55]. Spermine concentrations are relatively high in prostate tissue, while putrescine and spermidine are nearly absent. Therefore, spermine is the easiest and most important polyamine to consider during measurements [23].

1.5 Magnetic Resonance Spectroscopy

Magnetic resonance spectroscopy (MRS) provides biochemical information about metabolites in a defined volume of biological material. The examinations can be executed with most clinical magnetic resonance (MR) instruments with a field strength of 1.5 Tesla or higher.

1.5.1 Theoretical Basics of Magnetic Resonance Spectroscopy

The principles of MR are based on the variation of MR frequency when MR detectable nuclei in a strong magnetic field are hit by radio pulses. MR-sensitive nuclei are for instance phosphor, carbon and fluor. However, in clinical practice it is mainly the hydrogen core, hence a single proton, which is used [56, 57]. The MR-sensitive nuclei experience different chemical environments, as they are parts of different molecules. These distinct environments determine how well the cores are shielded from the outer magnetic field, and predict the resonance frequency for each core. The resonance frequency is normalized to be independent of the magnetic field strength, and subsequently named “chemical shift”, expressed in parts per million (ppm). A spectrum with the chemical shift of cores in different molecules on the x-axis and signal amplitude on the y-axis is produced from the collected data. The area under the curve is proportional with the concentration of cores in the tissue which is analyzed. Since protons in water and fat outnumber protons in other molecules by far, it is important that their signals are suppressed under data collection [56, 57]. A good quality, highly resolved spectrum consists of narrow, separated spikes, where each spike represents the cores of a molecule. Because each molecule produces a spike with a distinct form and chemical shift (placement along the x-axis), it is possible to recognize the different molecules in a tissue volume [56].

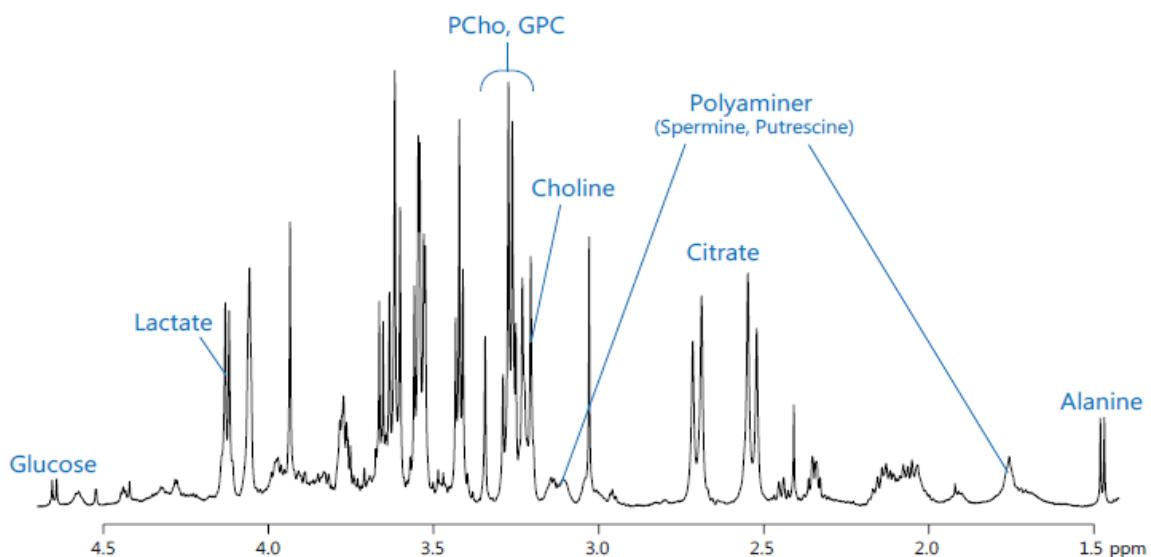


Figure 1.10: MRS spectrum of normal prostatic tissue.

1.5.2 *In vivo* Magnetic Resonance Spectroscopy

In vivo MRS can be separated into single-voxel and multi-volume, also called MRS imaging (MRSI), techniques. In single-volume, a defined volume is analyzed and a single spectrum is produced for the entire volume. With MRSI, several voxels in the same sequence are registered, and the biochemical information is presented in metabolic images overlaying normal anatomic MR images [57]. An *in vivo* spectrum can contain spikes made up of overlapping signals from several metabolites. For instance, it is not possible to separate between the different ChoCC. Their signals are overlapping and only one spike is visible, which is referred to as total choline (tCho) [57].

In vivo MRS is nowadays widely used in neurology, mostly in tumor diagnostics, but also increasingly in other conditions, such as epilepsy, multiple sclerosis, dementia and psychiatric diseases. Also in other medical fields, MRS is becoming a progressively important part of clinical practice. Especially for cancer diagnostics and follow-up, MRS has proven to be highly specific. In the US, incorporation of MRSI into routine MR examination of the prostate has been tested [57].

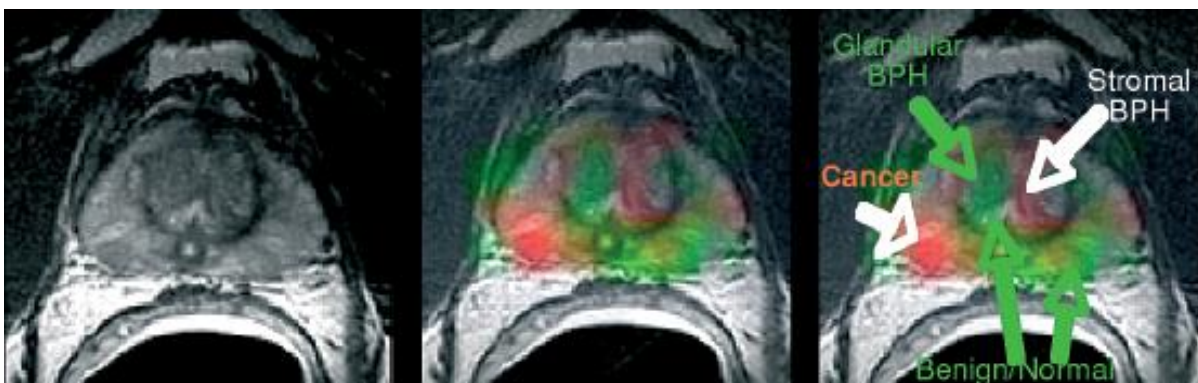


Figure 1.11: The picture to the left is a normal MR picture of the prostate. In the pictures in the middle and to the right, MRSI has been performed and added to the image. tCho is showed in red, while citrate is green. Areas with cancer have elevated ChoCC, hence there is a dense red color. Healthy areas are green, because of a high citrate content. The figure is reproduced from Gribbestad et al. [57].

1.5.3 High Resolution Magic Angle Spinning

Ex vivo MRS makes it possible to analyze tissue probes with a much higher magnetic field strength (7-21 Tesla) than *in vivo*, hence producing metabolic spectra of greater resolution [57]. A problem that emerges when analyzing intact tissue, such as surgical samples or needle biopsies, is that the MR-sensitive nuclei in the tissue are bound to each other and the metabolites are not able to change position. This leads to reduced resolution and peak broadening. In contrast, in fluid form *ex vivo* samples, nuclei can move freely and the problem of peak broadening is absent. A solution to the issue

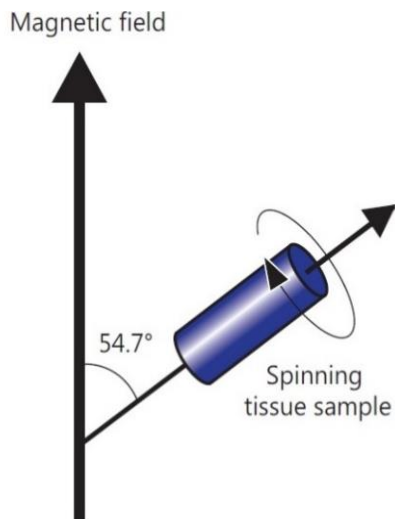


Figure 1.12: HR-MAS MRS tissue sample position

of examining intact tissue samples was found with a method called high-resolution magic angle spinning (HR-MAS), which can produce highly resolved spectra and detailed biochemical information despite the firm position of the nuclei. The method reduces the line broadening effect by placing the probe in the so called magic angle (54.7°) related to the magnetic field, and spinning it around its own axis with high speed (2-15 kHz, usually 2-5 kHz) [57].

Ex vivo HR MAS is today applied in a large extent in clinical studies on humane tissue, especially in research concerning brain, breast and prostate cancer [57]. HR-MAS has the advantage of giving exact information about biological tissue, and in addition leaving the samples unprocessed for subsequent histopathological evaluation or other molecular methods such as gene profiling [23, 58].

1.5.4 Magnetic Resonance Spectroscopy and Prostate Cancer

For PCa, a significant correlation between results from *ex vivo* HR-MAS analyses and *in vivo* MRSI of spatially matched regions has been confirmed [41]. It is of great interest to determine how findings from *ex vivo* MAS and *in vivo* MRS correlate, since this transmission of biochemical information opens new doors in cancer diagnostics and follow-up.

MRSI is already implemented into clinical practice in some hospitals, making use of the tCho+Creatine+Polyamines/citrate (CCP/C) ratio and the tCho+Creatinine/Citrate (CC/C) ratio. Both ratios increase in malignant prostate tissue [23, 59-61]. While the tCho can not be separated into its compounds *in vivo*, *ex vivo* HR-MAS of prostate biopsies makes it possible to distinguish between the ChoCC free choline, PCho and GPCho [50, 60, 62].

MRS, both *in vivo* and from *ex vivo* specimens, can measure the precise concentrations of metabolites in human tissue volumes. Variations in these concentrations have been successfully correlated with a number of diseases, including PCa [23, 40, 42, 61]. The decrease and increase of distinct metabolic markers have the potential to diagnose cancerous processes in the prostate, and provide information about cancer grade and aggressiveness. Therefore, MRS will play an increasing role in the diagnostic, follow-up and treatment of PCa.

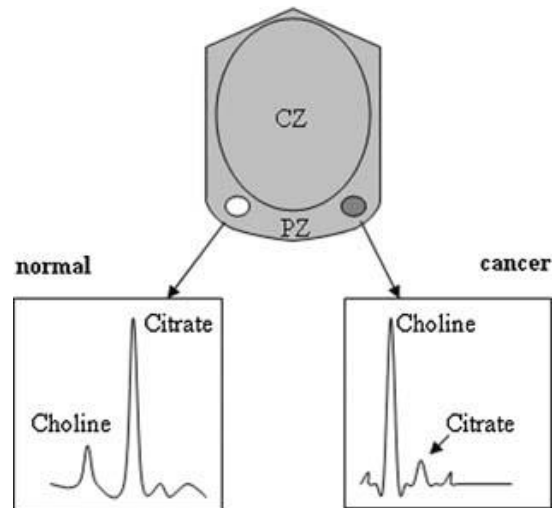


Figure 1.13: Alterations in metabolite concentrations in cancer compared to normal tissue presented in MRS spectra. The picture is obtained from Mycielska et al. [44]

1.6 Absolute Quantification of Metabolites by LCModel

Every metabolite gives rise to a particular spike, or set of spikes, in the MRS spectra. The metabolite concentration is proportional to the area under the spike (the curves integral). However, a HR-MAS spectrum of a tissue probe contains information about many metabolites, giving rise to overlapping signals. This makes the accurate quantification of individual metabolite peaks difficult [63]. Linear combination of Model spectra (LCModel) fits the obtained spectral data with a standardized set of metabolite spectra as a reference. The standardized spectra are obtained from pure, individual metabolite solutions. The metabolites included in the reference set are chosen according to the tissue of interest. After identification of the metabolites, quantification is performed by adding and comparing a known amount of a reference substance. By using a model of complete spectra instead of distinct spikes, it is possible to differentiate between metabolites that present similar peaks at one frequency in the spectrum [64, 65]. By identifying all of the peaks for each metabolite, more information about metabolites can be obtained and lower concentrations quantified. Besides, the lack of subjective handling of the spectra makes the metabolite results objective and replicable [66]. The LCModel was originally determined for *in vivo* spectra, but with adaption, it has proven to be applicable also in the quantification of *ex vivo* spectra [63]. Mostly, the model has been used in *ex vivo* MRS analyses of brain tissue, but also prostate material has been examined successfully [23, 65, 67].

1.7 Statistics

1.7.1 Linear Mixed Model

Linear mixed models (LMM) are general flexible approaches to analyze datasets containing correlated information. In situations with repeated measurements on the same subject or in different scenarios, each subject/scenario can affect the measurements in its own particular way [68, chapter 15]. The correlation patterns that arise, lead to a set of data that could lack independence. In many statistical methods, this lack of independent data leads to false results and meaningless p-values [69].

A LMM contains both fixed effects and random effects. Fixed effects have levels that are of primary interest and would be used again if the experiment were repeated, because they are known or suspected to affect the outcome of a study. Meanwhile, random effects also influence the outcome of a study, but are random and uncontrollable. By adding a random effect to the data obtained from each subject/scenario, LMM solves the problem of correlating data. For further understanding, linear models imagine the difference between the measured variables in a dataset as a linear function. While a simple linear model presents the analyses results as a single linear function, LMM allows each subject/scenario to get their own minor linear function with individual intercepts and/or slopes [68, chapter 15, 69]. This kind of model, mixing fixed and random effects to allow individual variability, has become an important statistical tool in almost every branch of science.

1.7.2 The Benjamini-Hochberg False Discovery Rate

When performing a large number of statistical comparisons on a set of data, some of the comparisons will obtain significant p-values (<0.05) simply by chance. Thus, multiple testing increases the occurrence of type I errors, where the null hypothesis is rejected even though it is true. This leads to false positive research findings. The problem of conducting multiple comparisons has become of growing interest in recent years as technological developments have made it possible to collect and analyze vast numbers of distinct variables, for instance in the testing of gene expressions [70]. Multiple testing corrections are statistical methods that recalculate the probabilities of test results obtained by multiple comparisons, thereby reducing the incidence of false positive findings.

One way to correct for multiple testing is the Benjamini-Hochberg (BH) procedure which was described by Benjamini and Hochberg in 1995 [71]. This method aims to control the false discovery rate (FDR), which is the proportion false positive test results. The individual p-values from each comparison are

put in order from smallest to largest. The smallest p-value gets the rank 1, the next gets the rank 2, etc. This makes the rank of the largest p-value the same as the total amount of p-values (N) [70]. Each original p-value is then multiplied by N and divided by its rank to obtain an adjusted p-value. A FDR can be chosen freely but is often set to 0.05. The adjusted p-values below the chosen FDR are considered true positive, making the results of their comparisons significant. However, test results with adjusted p-values greater than the FDR are insignificant and have to be rejected [72].

2 Purpose

In the recent years, stromal-epithelial interactions have proven importance for tumor development and progression. The tumor stroma enhances tumor growth, for instance by secreting growth factors and chemokines, and creates a microenvironment that is favorable for cancer progression. [17, 30]. In PCa, a desmoplastic response in the stroma surrounding the cancer foci can occur, and a method for grading the amount of response has been developed. RS has shown to be of prognostic value, independent of GS, PSA and other factors [17, 18, 32-34].

Metabolomics, the study of the metabolism in different cells, is an emerging field. The metabolism expresses the cell's phenotype, and is the result of all the processes within the cell, starting with the genotype. Hence, a cancer cell has a different metabolic profile than a normal cell, and identification and quantification of these profiles can provide valuable information about the nature of cancer. Several other studies have shown a correlation between metabolites like citrate, spermine and choline, and tumor aggressiveness [23, 40, 42, 61]. However, to our knowledge, no study has examined the correlation between RS and metabolism.

Our theory is that RS is an active tissue that contributes to cancer development and progression. Different RSGs predict dissimilar prognoses and survival rates, and with higher amounts of RS, the cancer appears more aggressive. Hence, the various RSGs must have differences in phenotypes, which should be expressed as alterations in the metabolism.

Our hypotheses are as follows:

1. Metabolic differences can be observed between different grades of RS.
2. Metabolic differences can provide information on which molecular pathways and metabolic markers are connected to RS and its grading.

3 Materials and Methods

3.1 Overview of Methods

This section gives a brief overview of the methods in the study. Tissue samples from radical prostatectomies were obtained from patients with PCa. These samples were harvested using a novel standardized method that will be discussed in more detail later in this chapter. Metabolic spectra were produced using HR-MAS and quantified by LCMoDel. The histopathology in the samples was evaluated regarding RS, GS and tissue composition. Statistical analyses were then used to investigate the correlation between metabolic concentrations and RSG.

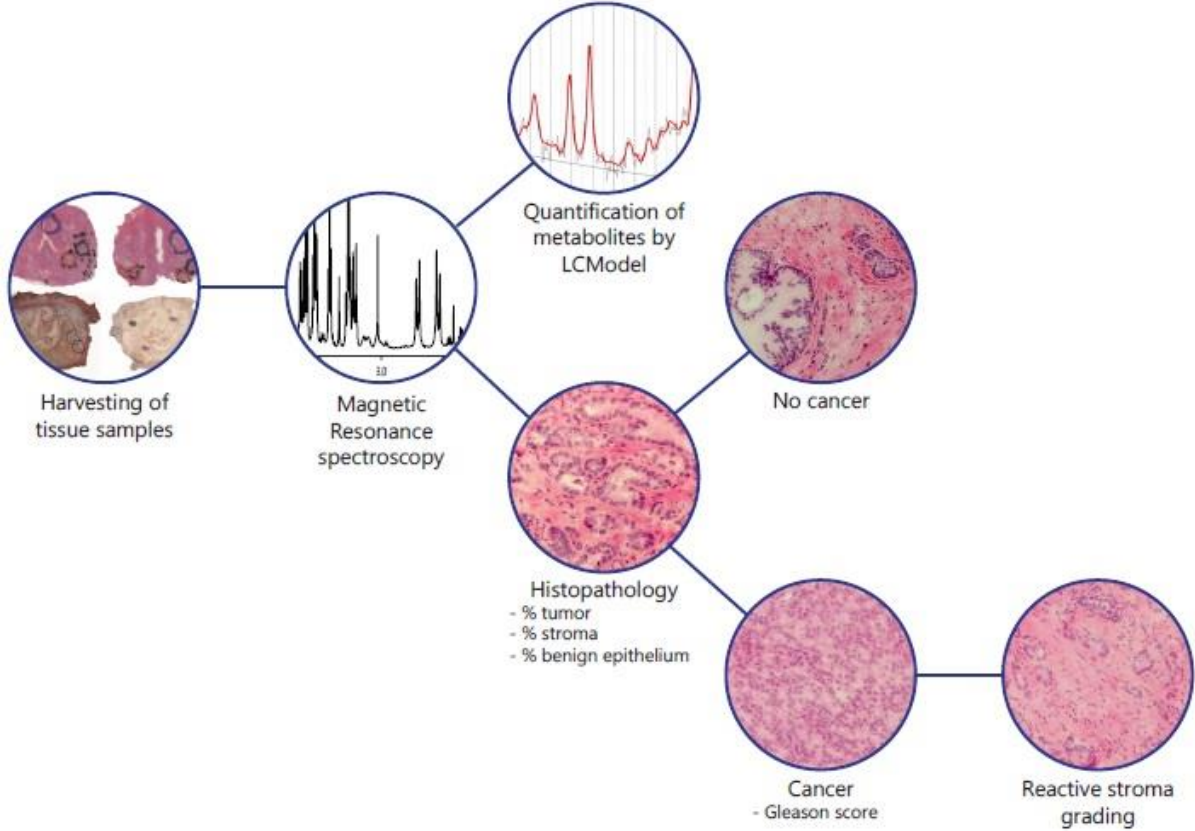


Figure 3.1: Overview of methods in this study. Picture of “Harvesting of tissue samples” is adapted from Giskeodegard et al. [23]. The picture of “Quantification of metabolites by LCMoDel” is adapted from Maltezos [73].

3.2 Patient and Tumor Characteristics

The prostate tissue samples in this study were obtained by Giskeodegard et al. [23], and came from 48 patients who underwent radical prostatectomy at St. Olavs Hospital, Norway from 2007. From each patient, a 2 mm transversal prostate tissue slice was collected for storage in the Regional Research Bank of Central Norway. All of the patients have signed an informed consent form. The Regional Committees for Medical and Health Research Ethics (REC) (reference number: 4.2007.1890/010-04) and the Data inspectorate of Norway have approved the study [23].

The 48 patients included did not receive any prostate cancer treatment prior to prostatectomy and had a tumor volume which made up >5% of the prostatic gland, estimated by histopathology [23]. Clinical patient characteristics are described in the table to the right (table 3.1).

Age (mean/range)	Years	62 (48-69)
sPSA (mean/range)	Before surgery	10.5 (3.7-45.8)
Tumor volume	Percentage of prostate gland	21 (5-90)
Gleason Score	3+3	1
	3+4	23
	3+5	1
	4+3	10
	4+5	10
	5+3	1
	5+4	1
	Unknown	1
Pathological T-Stage	T2a	2
	T2b	1
	T2c	29
	T3a	7
	T3b	7
	Unknown	2

3.3 Harvesting Method

The HR-MAS tissue samples were obtained by using a new harvesting method, described by Bertillon et al. [74]. On average 15 minutes after surgical removal of the prostate gland, a full tissue slice (2 mm) through the middle of the prostate, perpendicularly to the urethra, was obtained. The slice was photographed by a digital camera and immediately snap frozen by clamping it between two aluminium plates, precooled by fluid nitrogen. The tissue slice was put in a plastic bag for final storage at -80°C. Because of the rapid freezing of the prostate tissue, the original structure and metabolic composition is preserved. Hence, it is possible to evaluate the metabolic state [74]. The two remaining halves of the prostate gland were stitched to a cord board, in order to minimize the tendency for the capsule to retract during fixation, and avoid disturbances in histopathological evaluation of the surgical margin. After fixation in 4% buffered formaldehyde, both halves were further sliced (4 mm thick) and

embedded in paraffin. From each block, one section of thickness 4 μm was cut and stained with HES for diagnostic purposes [23].

3.4 Selection of HR-MAS Samples

In order to find areas with cancer in the fresh frozen prostate slice, the two HES-stained sections adjacent to the tissue slice were used to localize and grade cancer histologically. In the HES specimens, tumor areas were marked with a water resistant felt-tipped pen, differentiating between various Gleason grades by the use of predefined colors. Digital images of the scanned HES sections were fused with the photograph of the fresh frozen tissue slice. The final picture was printed on a transparent plastic sheet and projected over the frozen slice as a map to guide sample extraction. Cylindrical tissue samples (3 mm diameter) for HR-MAS were excised from regions with cancer tissue with different Gleason grades as well as normal prostate tissue (in total 162). Samples of normal prostate tissue were taken as far away from the cancer as possible. Several HR-MAS samples were obtained from each frozen slice (range 1-7 samples per slice (median: 3) depending on tumor size) [23, 74].

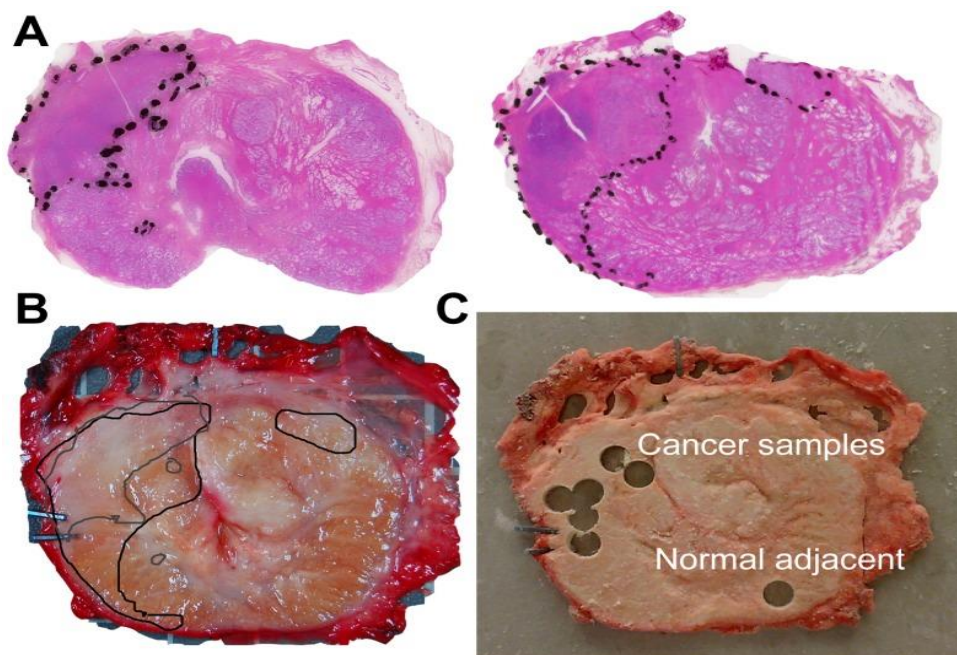


Figure 3.2: (A) HES-stained section adjacent to the frozen tissue slice. Regions of interest, both cancer and non-cancer, are marked with a water resistance felt-tipped pen (B) Fresh frozen tissue slice. The regions of interest have been transferred from the adjacent HES-stained sections by a transparent sheet. (C) Fresh frozen slice after HR-MAS sample extraction. The figure is adapted from Giskeodegard et al. [23].

A 4 μm cryosection was cut from one side of the extracted sample, HES-stained and evaluated by an uropathologist. This was done to determine the exact GS and tissue composition (percentage of cancer, stroma and benign epithelium) in the HR-MAS specimen. The prostate slices were placed on aluminium

plates in contact with fluid nitrogen during sample extraction to prevent the tissue from thawing and thus reduce molecular degradation. Hence, the HR-MAS samples were not thawed before the moment they were placed in the MR-magnet.

3.5 HR-MAS Experiments

Each prostate tissue sample (mean weight: 12.7 mg, range: 3.0-21.9) was moved to a HR-MAS insert with a sterile procedure described by Giskeodegard et al [23]. HR-MAS was executed on a Bruker Avance DRX600 (14.1 T) spectrometer (Bruker BioSpin, Germany) equipped with a $^1\text{H}/^{13}\text{C}$ MAS probe. Proton spectra were obtained by pulse-acquired spectra and by Carr-Purcell-Meiboom-Gill spin echo sequence, suppressing signals from lipids and macromolecules. The spectra were Fourier transformed, chemical shifts were referenced to the lactate peak (left peak of the doublet) and a linear baseline correction was applied. The human metabolomics database and previous published papers on HR-MAS in PCa were used to assign the peaks to the correct metabolites.

3.6 Quantification of Spectra by LCMoDel

The pulse-acquired spectra were quantified by LCMoDel using a novel basis set of 23 metabolites, thoroughly described by Giskeodegard et al [23]. The basis set was created using NMRSIM (Bruker BioSpin, Germany), where the desired metabolites were quantified between 0.8 and 4.7 ppm. The metabolite data obtained from HR-MAS was quantified according to added amount of formate. The concentrations obtained by LCMoDel are reported as mmol/kg wet weight [23].

3.7 Grading of Reactive Stroma

4 μm cryosamples, which were obtained and evaluated according to GS and tissue composition in Giskeodegard et al, were further examined [23]. The specimens were sent to another uropathologist, Elin Richardsen, for reactive stroma grading according to criteria found in previous articles [17, 18, 33]. RS grading is based on the amount of desmoplastic response in the stroma surrounding the epithelial tumor cells, hence, as the ratio between RS and cancer epithelium (figure 3.3): RSG 0: $\leq 5\%$ RS, RSG 1: 6-15% RS, RSG 2: 16-50% RS and RSG 3: $\geq 51\%$ RS and stroma-epithelial ratio of at least 1:1. Because our tissue samples were small (3 mm diameter), all of the stroma in the core was considered tumor stroma and needed to be examined for reactive changes. If epithelial cancer, but no reactive stroma was present, Richardsen graded the tissue sample as RSG 0 according to Saeter et al. In addition, she

evaluated whether the samples contained cancer tissue or not, GS, and the tissue composition (percentage of tumor tissue, stroma and benign epithelium).

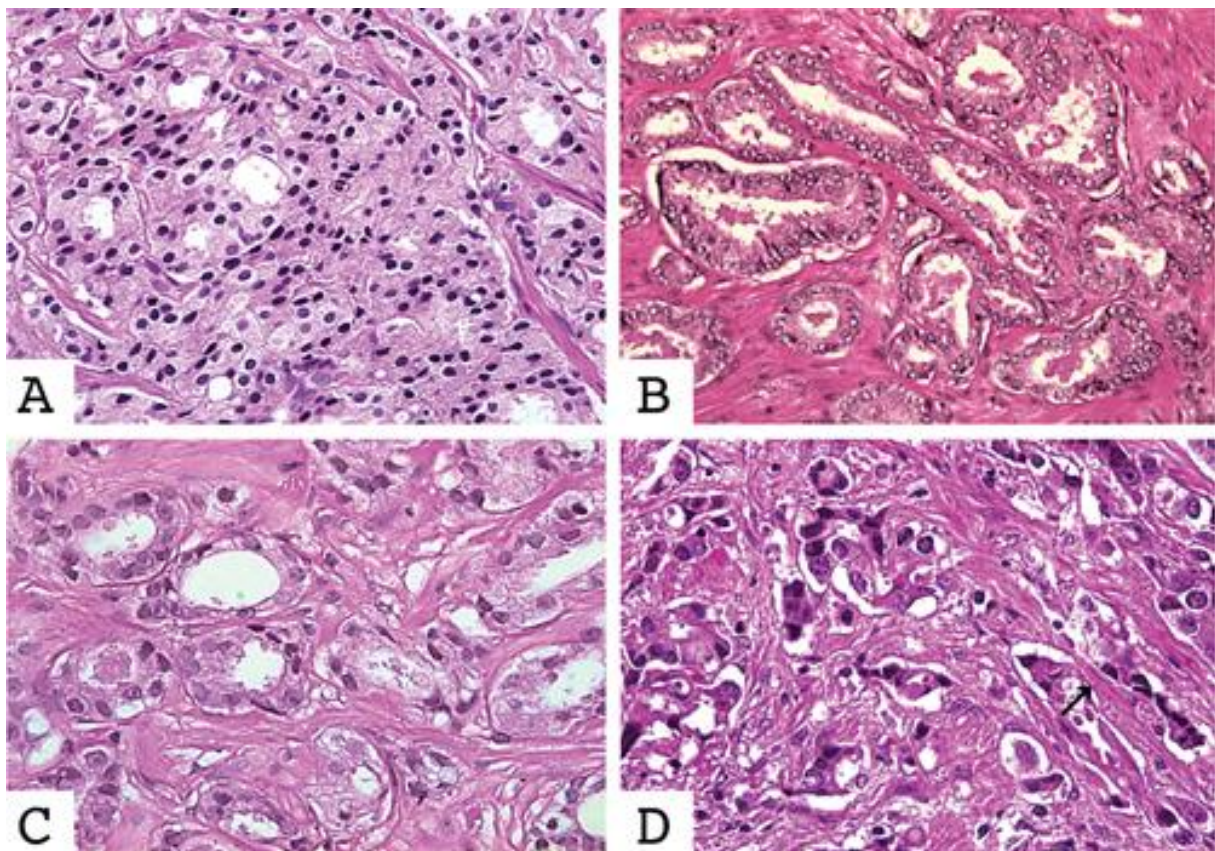


Figure 3.3: Reactive stroma grading in HES stained sections. **(A)** RSG 0: $\leq 5\%$ RS. Adenocarcinoma with GS 8. There is little or no RS in this sample. It should be noted that, in this case with a high GS, there is hardly any stroma at all. A cancer sample could just as well contain abundant stroma, but still be graded RSG 0 when there is no desmoplastic response observed. **(B)** RSG 1: 6-15% RS. GS 7. There is abundant stroma, most of it consisting of eosinophilic normal smooth muscle cells. However, some paler and more fibrillary areas with RS can be observed. **(C)** RSG 2: 16-50% RS. Adenocarcinoma with GS 7. The stroma is clearly paler and more fibrillary than in picture (B). **(D)** RSG 3: 51-100% RS. GS 9. The stroma appears pale and fibrillary, no smooth muscle cells are visible. The ECM forms a disorganized and fibrillary background pattern.

The figure is adapted from Saeter et al. [33].

3.8 Statistical Methods

3.8.1 Descriptive Statistics

The sample characteristics, RS, GS and tissue composition (percentage of tumor tissue, stroma and benign epithelium), were examined. Mean metabolite concentrations \pm SD were obtained for benign tissue samples and for each RSG. Descriptive analysis of the dataset was performed in SPSS (IBM, SPSS Statistics, USA).

3.8.2 Linear Mixed Model

As mentioned, several tissue samples were gained from each patient. To adjust for intrapatient correlation of metabolic concentrations, the patient variable was added to the LMM as a random effect. LMM analysis was performed in R (R Development Core Team, GNU General Public Licence).

Prior to LMM analysis, the metabolite concentrations were log transformed in SPSS with the formula $LOG(\text{metabolite} + 0.05)$ to obtain normal distribution. For six metabolites, normal distribution was not possible, because of too many zero concentrations. This applies for putrescine, ethanolamine, phosphocholine, isoleucine, glyserophosphoethanolamine and glucose. However, they were analysed with LMM in the same manner as the remaining metabolites. It is important to note that LMM is a statistical model that assumes normal distribution of the dependent, measured variable; in this case metabolite concentrations. Therefore, the results from the six metabolites which were not normally distributed, must be interpreted with caution. If however, the model's residuals are normally distributed for one of these metabolites, it's concentrations are close enough to normal distribution to make the LMM work properly. The distribution of residuals can be checked with a QQ-plot, which was produced for all the significant metabolites lacking normal distribution.

The aim of our analyses was to investigate the relationship between metabolite concentrations and different grades of RS in our tissue probes. Therefore, our focus was on cancer samples only, and the main analyses were performed on this dataset (n= 104). Nevertheless, the whole mount of samples (n=149) was investigated in a similar manner to check if adding non-cancer samples to the dataset would affect the results significantly.

There are several other factors in addition to RSG which may add variation to the dataset, and must be accounted for in the analysis. GS and the percentages of tumor, stroma and benign epithelium, were all suspected to affect the concentrations of the tested metabolites. To examine the significance of these factors in the analysis, each factor was included in a LMM individually. The script was set up as follows, and the dataset included cancer samples only:

Metabolite concentration ~ RSG + influencing factor + (1|patient) (1)

A p-value describing the influence of each factor on the RSG-metabolite relationship was obtained for each metabolite. After correction for multiple testing, the percentage of benign epithelium in the samples was found to be of no significance. GS, tumor and stroma percentage in contrast, were significant additions to the LMM for some of the metabolites. Since most of the metabolites were affected by these factors, a final script including GS, tumor and stroma percentage was used for analyzing all metabolites:

Metabolite concentration ~ RSG + GS + Tumor percentage + Stroma percentage + (1|patient) (2)

The influence of each fixed effect on metabolite concentrations in the final script (2) can be viewed in the appendix (table 7.4). After the LMM analyses, p-values were adjusted for multiple testing, using the Benjamini-Hochberg FDR multiple testing correction by usage of the *p.adjust (set of p-values, method="BH")* function in R.

The metabolites citrate and spermine are secreted into the lumen of the prostatic ducts. Hence, the luminal space (LS) affects the amount of metabolite in the tissue. Cancer progression can repress the ductal system, thereby reducing the LS. We had measurements of LS for 126 of our samples (n= 92 for cancer samples only). The influence of LS on the relationship between citrate and spermine concentrations and RSG was investigated by including LS measurements for the 92 cancer samples into the LMM with the following script:

Metabolite concentration ~ RSG + LS + (1|patient) (3)

In this formula, LS proved significant for both citrate (p= 0.0010) and spermine (p=0.0011). Therefore, LS was included as a factor into the LMM when analyzing citrate and spermine. Since the dataset with LS measurements contained fewer samples, LS was added to the LMM for citrate and spermine after the main script was executed.

4 Results

4.1 Histopathology

There were 158 histopathological HES samples and 151 corresponding metabolic profiles of the core biopsies. Hence, seven histopathological graded samples had to be removed from the dataset. Additional two samples were excluded because of incorrect histopathological grading. Therefore, in total 149 samples were used in the statistical analyses.

Of the 149 samples, 104 contained cancer, while 45 were benign (table 4.1). The distribution of high ($\geq 7b$) and low ($\leq 7a$) GS was relatively even in the cancer samples (table 4.1). RS was graded in the 104 cancer samples (table 4.2), but the amount of samples within each grade varied greatly (table 4.1, figure 4.1A). RSG 3 was present in only six of the tissue samples, while RSG 1 represented almost 40% (56.7% of cancer samples) (table 4.1, figure 4.1A). However, the different RSGs were almost equally distributed between high and low GS (figure 4.1B).

		Frequency	Percentage
Cancer/no cancer	Cancer	104	69.8
	No cancer	45	30.2
Reactive Stroma Grade	RSG 0	23	15.4
	RSG 1	59	39.6
	RSG 2	16	10.7
	RSG 3	6	4.0
	no cancer/normal stroma	45	30.2
Gleason Score	3+3	29	19.5
	3+4	24	16.1
	3+5	2	1.3
	4+3	16	10.7
	4+4	14	9.4
	4+5	10	6.7
	5+3	1	0.7
	5+4	8	5.4
	0	45	30.2

		Frequency	Percentage
Low ($\leq 7a$) vs. high ($\geq 7b$) GS	low GS	53	35.6
	high GS	51	34.2
	no cancer	45	30.2
		Mean	Range
Tissue composition	Tumor percentage	43,6	(0-100)
	Stromal percentage	36,2	(0-100)
	Benign epithelium percentage	20,2	(0-80)

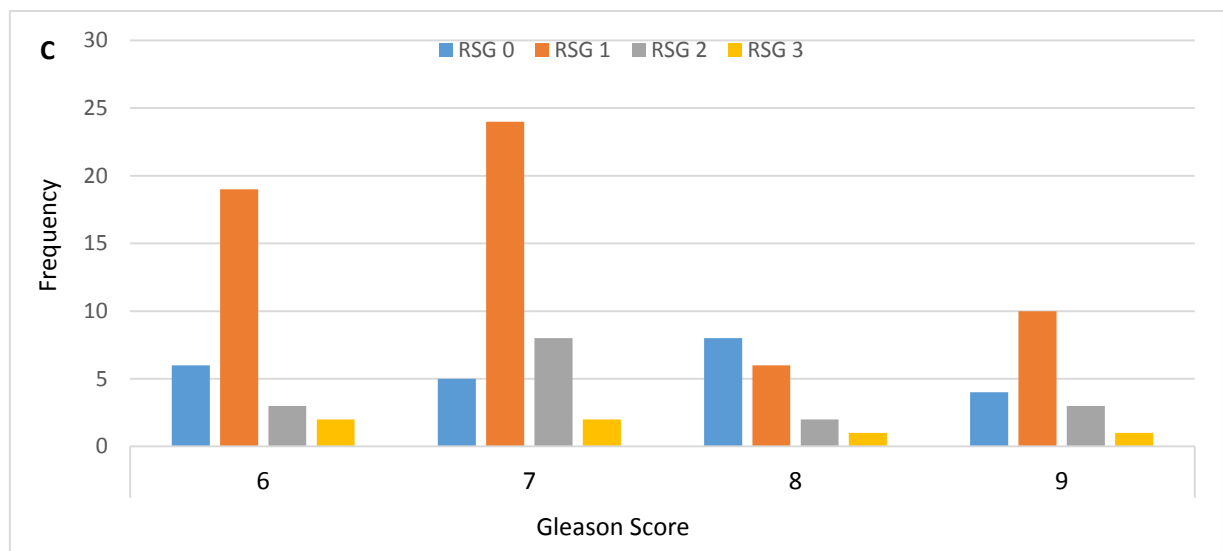
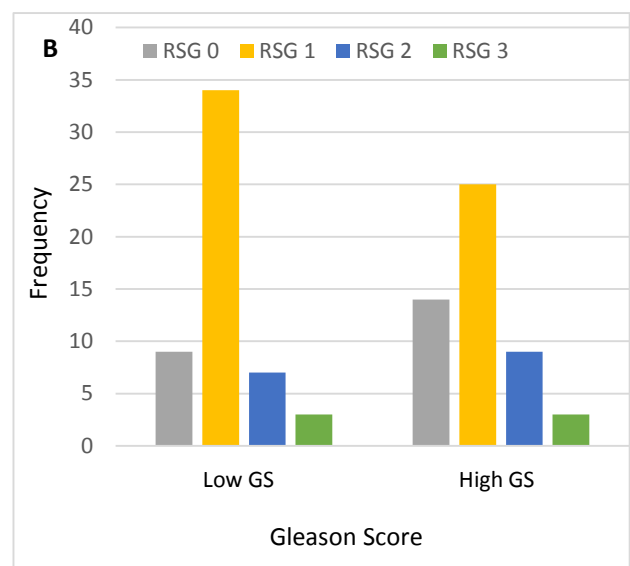
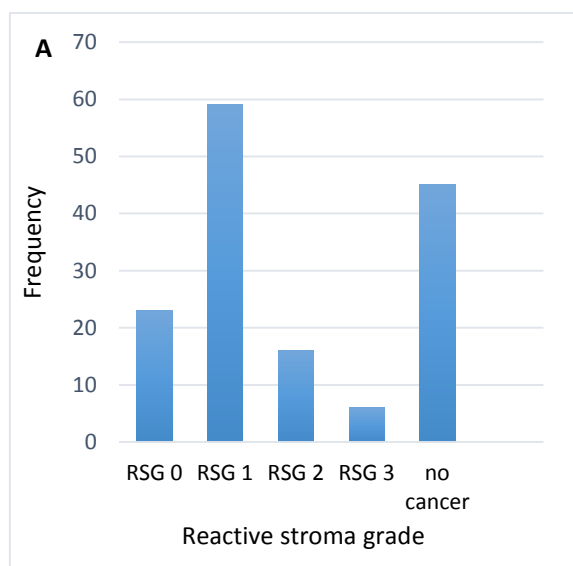
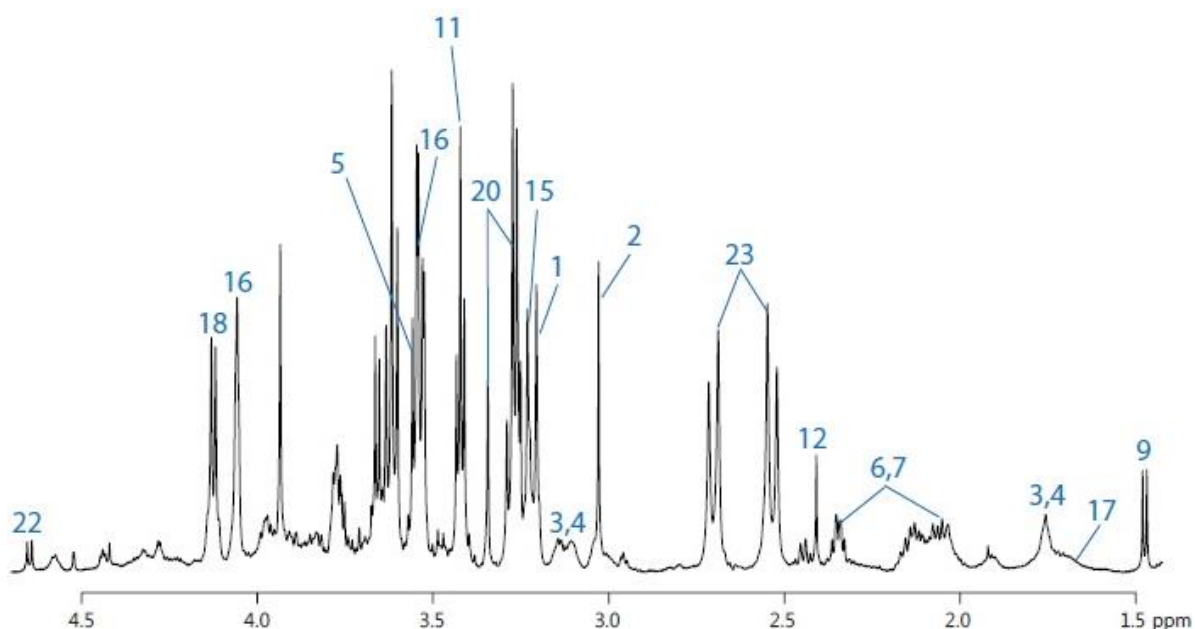


Figure 4.1: (A) Distribution of RSG in the whole mount of tissue samples. RSG 1 makes up the majority, while only six samples were graded RSG 3. (B) Distribution of the four RSGs between low ($\leq 7a$) and high ($\geq 7b$) GS. RSG is very evenly spread, with three samples graded RSG 3 in each group. (C) Distribution of RSG between each GS.

4.2 Overview of quantified Metabolites

The following HR-MAS spectrum is an example of a spectrum produced of normal prostate tissue (figure 4.2). It shows the position of the majority of the 23 metabolites presented in this study. Our basis set of metabolites is presented in the table below the spectrum (figure 4.2).



Assg.	Metabolite	ppm	Assg.	Metabolite	ppm
1	Choline	3.13	13	Scyllo-Inositol (na)	3.34
2	Creatine	3.04	14	Phosphoethanolamine (na)	3.24
3	Spermine	1.78, 3.15	15	Phosphocholine	3.21
4	Putrescine	1.75, 3.04	16	Myo-Inositol	3.54, 4.06
5	Glycine	3.55	17	Leucine	1.80
6	Glutamine	2.14 - 2.31	18	Lactate	1.34, 4.11
7	Glutamate	2.09 - 2.34	19	Isoleucine (na)	1.96
8	Ethanolamine (na)	3.13	20	Glycerophosphocholine	3.32
9	Alanine	1.47	21	GPEA* (na)	3.20, 4.10
10	Valine (na)	1.92	22	Glucose	5.24
11	Taurine	3.41	23	Citrate	2.55, 2.70
12	Succinate	2.39			

Figure 4.2: HR-MAS spectrum of normal prostate tissue. The basis set of metabolites used in this study is presented in the table. The metabolites are assigned to peaks in the spectrum by numbers. Metabolites marked with (na), are not placed in the spectrum. Ppm values are only approximate and most of the metabolites have more peaks than listed.

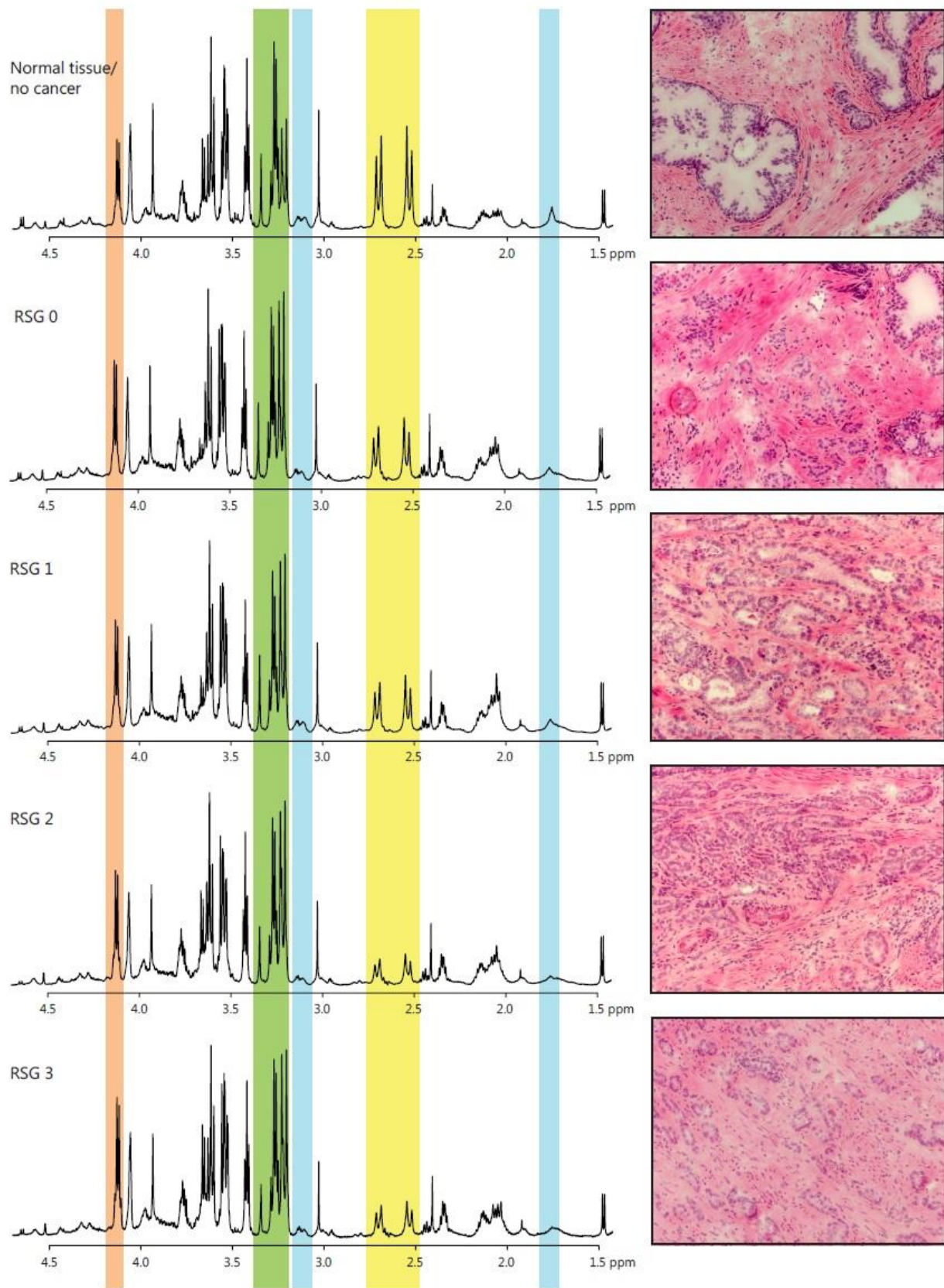
*GPEA: glycerophosphoethanolamine

4.3 Metabolic Changes between different Reactive Stroma Grades

Mean values of metabolite concentration (mmol/kg) for each RSG are presented in the table below (table 4.2).

Metabolite	No cancer	RSG 0	RSG 1	RSG 2	RSG 3
Choline	0.5769 (0.4917)	1.1456 (0.8599)	1.1529 (0.6931)	1.3848 (0.8292)	1.2392 (0.3950)
Creatine	2.4402 (1.1048)	2.2870 (0.8341)	2.0877 (0.7443)	2.4220 (0.6698)	2.0337 (0.6190)
Spermine	2.6304 (3.1873)	1.8308 (1.2220)	1.9755 (2.4172)	1.3408 (1.5326)	0.8781 (0.3765)
Putrescine	0.7648 (1.1469)	0.3865 (0.6048)	0.2159 (0.3551)	0.1506 (0.2785)	0.0311 (0.0762)
Glycine	1.8060 (1.7215)	2.6124 (1.2993)	2.5207 (1.1215)	2.9417 (1.1812)	2.4700 (0.3738)
Glutamine	2.1147 (1.0273)	3.1099 (1.1974)	2.8214 (1.0668)	3.2248 (1.4976)	2.8091 (0.6452)
Glutamate	2.9199 (1.3973)	5.7260 (3.4169)	5.2182 (2.2941)	5.7014 (2.2315)	5.3110 (1.1611)
Ethanolamine	0.5208 (1.6690)	0.2093 (0.3269)	0.1919 (0.3988)	0.0891 (0.2249)	0.0243 (0.0595)
Alanine	1.8761 (1.2993)	2.2111 (0.8922)	2.2213 (0.8894)	2.9337 (1.3079)	2.3685 (0.9205)
Valine	0.3430 (0.6726)	0.5310 (0.5241)	0.4216 (0.2873)	0.4575 (0.2952)	0.3791 (0.0981)
Taurine	5.4337 (2.4983)	5.3146 (2.0466)	4.5748 (1.7433)	6.1444 (2.3854)	5.7767 (1.6510)
Succinate	0.4900 (0.5859)	0.6340 (0.2912)	0.6425 (0.3166)	0.7010 (0.2419)	0.6058 (0.0920)
Scyllo-Inositol	0.5185 (0.6706)	0.4914 (0.3460)	0.5266 (0.3522)	0.5091 (0.3239)	0.4030 (0.1876)
Phosphoethanolamine	1.8116 (0.9776)	2.4220 (1.2170)	2.6770 (1.2209)	3.4754 (1.0682)	3.0858 (0.9855)
Phosphocholine	0.3741 (0.2737)	0.6529 (0.3842)	0.7833 (0.5621)	1.0418 (0.4565)	0.8474 (0.3644)
Myo-Inositol	9.6220 (4.9232)	10.0011 (3.6518)	9.2167 (3.2233)	9.8952 (2.0278)	10.0460 (2.1283)
Leucine	0.2813 (0.2049)	0.7209 (0.7435)	0.5703 (0.5395)	0.7202 (0.7183)	0.5593 (0.2275)
Lactate	13.4655 (6.2319)	19.9984 (8.0446)	18.8537 (7.8950)	20.9126 (5.7145)	22.4026 (3.3866)
Isoleucine	0.0986 (0.1075)	0.1898 (0.1499)	0.1921 (0.1507)	0.1704 (0.1617)	0.1828 (0.1267)
Glycerophosphocholine	0.4235 (0.2493)	0.9180 (0.8272)	0.9073 (0.7188)	1.2552 (0.7372)	0.9840 (0.5284)
Glycerophosphoethanolamine	0.2691 (0.2644)	0.5660 (0.9673)	0.3955 (0.6348)	0.1563 (0.3403)	0.2251 (0.2588)
Glucose	1.1585 (1.0838)	0.6641 (0.7145)	0.1741 (0.3374)	0.1711 (0.3465)	0.2986 (0.3528)
Citrate	11.7283 (10.8791)	8.3200 (3.5345)	8.0253 (6.9287)	5.4275 (4.0370)	4.5543 (2.6708)

*Standard deviations are presented in parenthesis



Lactate	ChoCC (Choline, PCho, GPC)
Polyaminer (Spermine, Putrescine)	Citrate

Figure 4.3: The average metabolic spectra from each RSG and normal tissue are presented with histopathological examples. Metabolites of interest are marked in different colors and presented in the legend to the left. Note that the HES picture demonstrating benign prostate tissue shows some degree of hyperplasia.

4.4 Metabolic Changes Regarding Reactive Stroma Grade with LMM

The correlation between metabolite concentration and RSG was investigated in cancer samples (n=104) and adjusted for GS, tumor and stroma percentage. The patient variable was added as a random effect. The significance of RSG for metabolite concentration can be viewed in the table below (table 4.3). P-values before and after correction for multiple testing are displayed. In addition, the factors influencing the relationship between metabolite concentration and RSG were added to the LMM one by one. Their effect on the significance of RSG can be viewed in the appendix (table 7.1).

Metabolite	p-value before BH	p-value after BH
Choline	0.1398	0.4542
Creatine	0.5941	0.7592
Spermine	0.2364	0.4542
Putrescine*	0.2370	0.4542
Glycine	0.4438	0.6005
Glutamine	0.8496	0.8882
Glutamate	0.4300	0.6005
Ethanolamine*	0.0373	0.2858
Alanine	0.3335	0.5113
Valine	0.9879	0.9879
Taurine	0.7263	0.8352
Succinate	0.1571	0.4542
Scyllo-Inositol	0.2794	0.4943
Phosphoethanolamine	0.0580	0.3337
Phosphocholine*	0.1691	0.4542
Myo-Inositol	0.6985	0.8352
Leucine	0.2011	0.4542
Lactate	0.3211	0.5113
Isoleucine*	0.7698	0.8431
Glycerophosphocholine	0.2086	0.4542
Glycerophosphoethanolamine*	0.1330	0.4542
Glucose*	0.0100	0.1150
Citrate	0.0071	0.1150

Significant values are marked with yellow. Borderline significant results are written in red.
*the metabolite does not have a normal distribution.

Ethanolamine (p=0.0373), glucose (p=0.0100) and citrate (p=0.0071) concentrations were initially found to significantly vary with different grades of RS. However, after correction for multiple testing, none of them remained significant. Still, these metabolites were examined further by investigating the exact factors influencing their concentrations.

4.4.1 Adjusted Models for Ethanolamine and Glucose

For ethanolamine, only RSG proved to affect metabolite concentration significantly. A new LMM considering only RSG and inpatient correlation was performed and the correlation between RSG and ethanolamine concentration was strengthened ($p=0.0299$).

Glucose concentration was significantly correlated to RSG and stroma percentage. In a new LMM adjusted for only these factors and the inpatient correlation, the significance of RSG for glucose concentration increased ($p=0.0068$).

However, neither ethanolamine nor glucose were normally distributed. When inspecting residual QQ-plots of the two metabolites (figure 4.4A and B), apparent deviations from normality were observed. This suggests that the assumption of normality required by LMM was not met for ethanolamine and glucose, and their correlation to RSG could not be confirmed. Therefore, we will not discuss these metabolites any further.

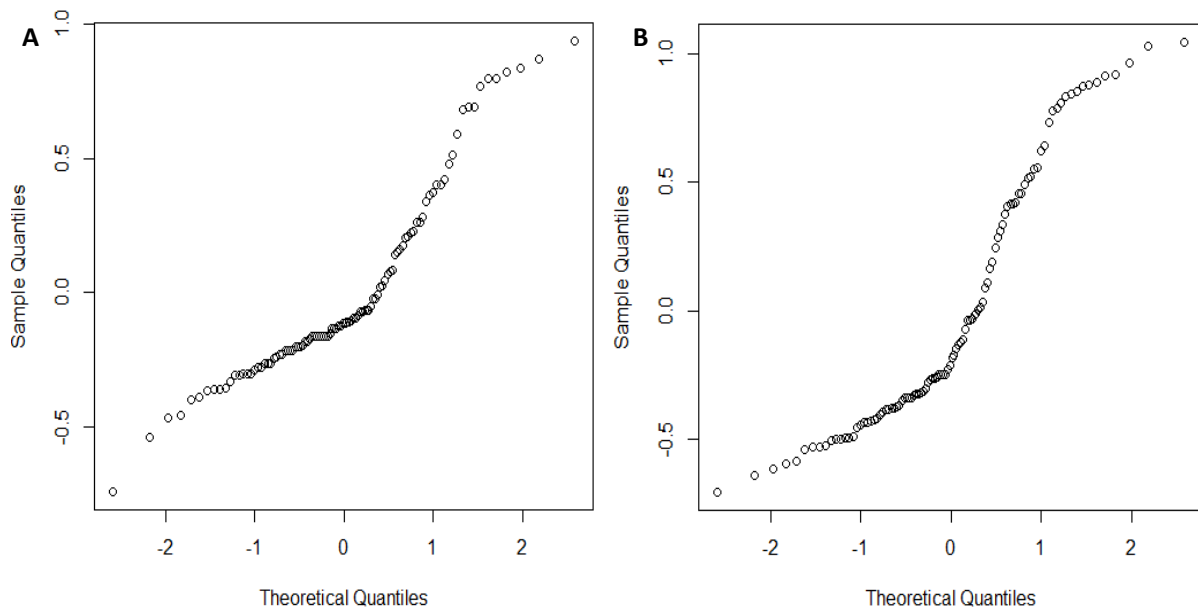


Figure 4.4: (A) Residual QQ-plot of ethanolamine. (B) Residual QQ-plot of glucose.

4.4.2 Adjusted Model for Citrate

Citrate concentration was significantly dependent on RSG and GS. A new model, taking only these two factors and inpatient correlation into consideration, strengthened the correlation between citrate concentration and RSG ($p=0.0043$). Intercepts and standard errors of the new model can be viewed in the table to the right (table 4.4). As

	Value	Standard Error
Intercept	1.8892	0.2002
RSG	-0.0976	0.0328
GS	-0.1419	0.0269

mean concentrations of citrate for different RSGs (table 4.2) and the average spectra (figure 4.3) indicate, the LMM proves that citrate concentrations decrease with increasing RSG.

4.4.3 Adjusting for Luminal Space

LS was found significant for citrate and spermine concentrations. Therefore, to obtain the correct picture of their correlation to RSG, LS had to be adjusted for. As spermine concentrations did not show significant differences

	Value	Standard Error	p-value
Intercept	1.5113	0.2252	1.5544E-08
RSG	-0.0818	0.0317	0.0127
GS	-0.1029	0.0289	8.0913E-04
LS	1.1908	0.3868	0.0035

between the grades of RS, no further analyses regarding spermine were performed. For citrate, LS was added to the customized model containing RSG, GS and patient variability. Citrate concentrations were still found to correlate significantly to RSG ($p=0.0127$). Intercepts, standard errors and p-values of the complete citrate model can be viewed in the table above (table 4.5).

4.4.4 Metabolic changes regarding RSG when considering all Samples

The correlation between metabolite concentration and RSG was investigated in the whole mount of tissue samples ($n=149$). The same LMM formula, adjusted for GS, tumor, stroma percentage and inpatient correlation, was applied. Non-cancer samples were given an individual RSG to fit these samples into the model and to separate them from RSG 0.

Significant differences in concentrations of spermine ($p=0.0082$), phosphocholine ($p=0.0273$), leucine ($p=0.0381$) and citrate ($1.5895E-04$) were observed. However, after correction for multiple testing, only citrate remained ($p=0.0037$) significant and spermine showed borderline significance ($p=0.0938$). The complete set of p-values obtained in this analysis can be viewed in the appendix (table 7.2).

4.5 Summary of Citrate Changes

When looking at the mean values and average spectra, there is an apparent decline in citrate concentration from benign tissue to cancer, and with increasing RSG (table 4.2, figure 4.3). This is also reflected in the LMM analyses where RSG shows significance for citrate concentration ($p=0.0071$). The p -value after BH correction, however, did not remain significant ($p=0.1150$). A customized LMM, performed with the cancer samples, only including the factors that have proven to affect citrate concentrations (GS, LS), still showed citrate concentration to differ significantly with RSG ($p=0.0127$). Considering all tissue samples, there was a significant difference in citrate concentration between RSGs and non-cancer samples ($p=1.5985E-4$). These results remained significant after correction for multiple testing.

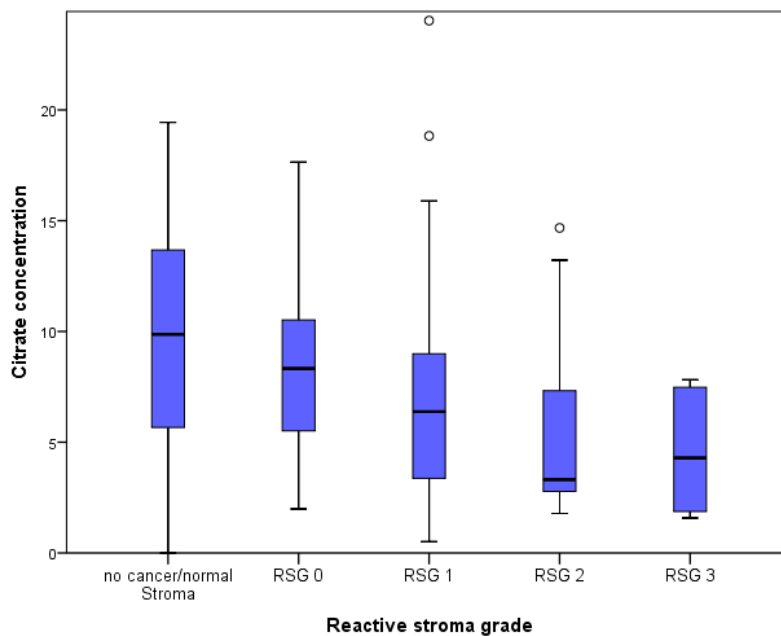


Figure 4.5: Boxplot of citrate concentrations in normal stroma and different grades of RS. The median concentrations are marked by black lines. Some of the outlying values are not shown in the plot as their concentration is above the limit set for the y-axis.

5 Discussion

5.1 Reactive Stroma and Metabolomics

In the last years, RS has acquired increased attention due to its importance regarding cancer growth and progression [30]. Several studies have tried to explain the changes that occur in the stroma as a reaction to PCa, but still many of the metabolic pathways and their alterations remain unknown [30, 31]. The grading of RS has proven to be a predictive factor for PCa recurrence and mortality, with increasing amounts of RS leading to a poorer prognosis [17, 18, 32]. Even though RSG often correlates with clinicopathological parameters, such as PSA, T-stage and GS [18, 34], some studies have been able to prove RSG as an independent prognostic factor [17, 18, 33]. This means that the amount of desmoplastic response in the PCa stroma by itself affects cancer behavior and predicts the development of the disease. We have previously explained how RS, through signaling molecules and ECM remodeling, creates a favorable microenvironment for cancer cells to proliferate and migrate. Therefore, metabolic processes and signal pathways in the stroma itself hold important information for the understanding of PCa. As increasing RSG leads to higher incidence of PCa specific mortality [33], there has to be an altered metabolic activity not only between normal stroma and RS, but also between the different grades of RS. Hence, it should be possible to detect differences in the metabolic profiles of these tissue groups.

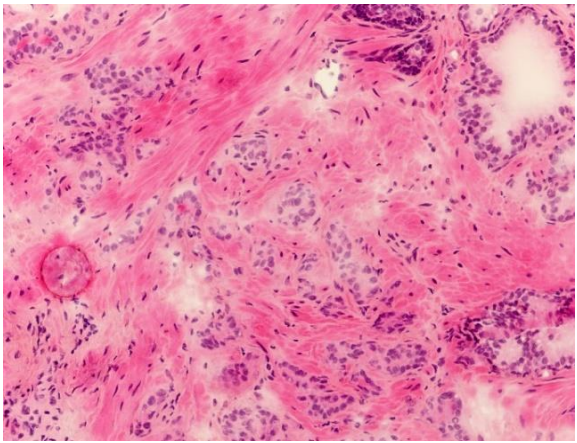
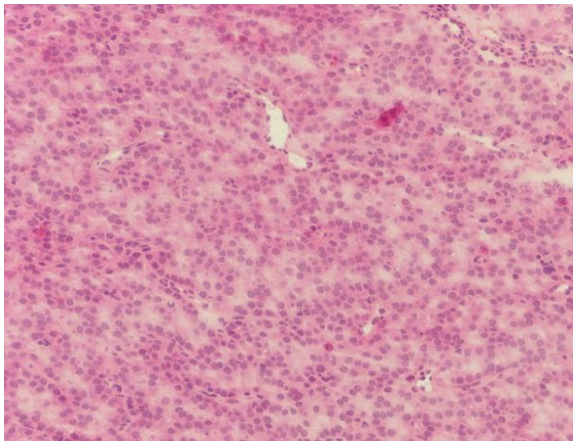
5.2 Importance of Different Reactive Stroma Grading Systems

Pathologist Elin Richardsen graded the RS in this study, using previous articles on the subject as a reference when evaluating the samples [17, 18, 32, 33]. While the concern of these articles is the correlation between RSG, cancer aggressiveness and prognosis, our study focused on the metabolic profile of each RSG. Regarding the grading of RSG 0 there are some discrepancies in the articles because of different grading criteria. Therefore, we will now discuss these differences and why we have chosen to use the method of Saeter et al.

Saeter et al.[33] found a significant correlation between GS and RSG. Low GS samples had a large percentage of RSG 0. With increasing GS the amount of RSG 0 decreased, while RSG 2 and RSG 3 increased. However, independent of GS and other clinical parameters, they stated that RSG can predict PCa associated mortality. The higher the RSG, the poorer is the prognosis [33]. Earlier studies have also shown a correlation between RSG and cancer mortality, but not the same correlation with GS. Ayala

et al.[32] and Yanagisawa et al.[17], which have published some of the first articles on the subject, found that cancer with minimal RS (RSG 0) or abundant RS (RSG 3) had a worse prognosis than RSG 1 and 2. The reason for this discrepancy could be that the studies have chosen to grade RSG 0 in different manners. Saeter et al. graded their samples as RSG 0 when there was no desmoplastic response present. Hence, many of the low-grade cancers received RSG 0. In contrast, Yanagisawa et al. chose to refrain from grading a sample as RSG 0 when there was no RS and only small tumor foci present. Instead, these samples were graded as RSG 1. Thereby, most of the probes with RSG 0 contained aggressive cancer with high GS, which had and only a small stromal component in general. This could explain why Yanagasawi et al. found RSG 0 to be a negative predictor for biochemical recurrence free survival, opposed to Saeter et al.

We chose to grade our samples in the same manner as Saeter et al. because this agrees with our theory of RS as an active contributor for cancer development. Hence, the more epithelial-stromal interaction there is in the tissue sample, the more aggressive and malign the cancer. Consequently, RSG 0 can be present both in high and low-grade cancer, like shown in the table below (table5.1).

Table 5.1: The occurrence of RSG 0 in both high grade and low grade cancer	
(A) RSG 0 and GS 6	(B) RSG 0 and GS 8
	
<p>Both of the HES stains above are graded RSG 0, but there are obvious differences in the tissue architecture. (A) The tissue sample has a low GS and abundant stroma. However, there is no RS present. The stroma has a normal appearance, with bundles of eosinophilic smooth muscle. (B) High GS. There is no normal glandular architecture in this sample. The epithelial cells are the completely dominating component, and there is a general lack of stroma. Hence no RS is observed and the sample is graded RSG 0.</p>	

These differences in the grading system influence the distribution of RSG between different GS. However, when looking at how our samples vary with high and low-grade GS, they show the same pattern of distribution in both blocks (figure 4.1B). This does not correspond to the RS-GS correlation we first assumed. Considering the Saeter et al. grading method, there should be an increasing amount

of RSG 3 with increasing GS. However, in our samples an equal amount of RSG 3 is found in low grade, compared to high grade PCa. In addition, when considering each GS separately, only the amount of RSG 1 seems to vary between the GS, while the other RSGs are evenly distributed (figure 4.1C). RSG appears to be independent of GS in our samples, which might be positive considering our statistical analyses. First, because this independence increases the probability of RSG contributing additional information to today's prognostic tools. Second, in LMM different fixed factors should correlate as little as possible for the model to work properly. Therefore, if RSG and GS were to have a strong correlation, RSG would have little additional information to contribute to the predictive model. When performing LMM we adjusted for GS, because even though there was an apparent visual independence between RSG and GS, metabolite concentrations were significantly influenced by GS.

5.3 Metabolite Changes in Reactive Stroma

5.3.1 Citrate

Our results showed that citrate concentration was significantly correlated to RSG before correction for multiple testing was performed. The concentration decreases with increasing RSG. Earlier we described the alterations in the metabolic pathways in PCa cells that lead to a decreased level of citrate. This change can be seen early in cancer development and can therefore serve as a biomarker for PCa [43]. Giskeodegard et al. [23] have also shown a correlation between high GS and decreased citrate levels, using *ex vivo* HR-MAS MRS. These results seem to be logical, as GS is description of the epithelium, which are the cells responsible for the production and secretion of citrate. Therefore, 58% of the variance in tissue citrate can be explained by the volume of normal citrate producing epithelium [51]. However, we did not find benign epithelial volume to be a significant contributor for citrate concentrations. Also, after adjusting for GS, tissue composition and luminal space alterations, we found RSG to be an independent factor for citrate concentration, even though the stroma is not producing this component. An explanation for this finding could be that the desmoplastic reaction is influencing the epithelial cells in a manner that changes their metabolic activity, hence the citrate concentration. Previously, we have described RS and the reciprocal cell-to-cell interaction with the cancerous epithelium, e.g. by secreting growth factors and chemokines [30, 33]. How these interactions work in detail is still unknown and needs further investigation. However, a lot of information about the metabolic alterations inside a PCa cell is identified. While normal prostate cells accumulate and secrete citrate, this ability is lost in the PCa cell. Zinc transporters are down regulated, thereby reducing the intracellular zinc levels and the inhibition of the enzyme ACON ceases. Further, the increased activity of ACON leads to less citrate accumulation and more energy production through the TCA cycle. In addition, citrate is used in lipid and cell membrane synthesis, which further reduces

the citrate levels [40, 43, 45]. Our results indicate that RS might influence this process, but in what manner is still undetermined.

5.3.2 Spermine

Spermine is a natural polyamine, together with spermidine and putrescine. These polyamines play a role in the regulation of cell proliferation and differentiation [52]. Spermine has been demonstrated to have an inhibiting effect on PCa cell growth [51]. Hence, it is reasonable that higher levels of spermine have been found in benign tissue compared to cancer [52, 55]. Previously, the levels of spermine have been shown to correlate with the amount of normal prostatic epithelium, which makes it possible to assume that spermine is produced by the epithelial prostatic cells [51]. Giskeodegard et al. also found a correlation between decreasing spermine levels and increasing tumor aggressiveness [23].

When looking at our entire dataset (n=149), also including non-cancer samples, we found that there was a significant correlation between spermine concentrations and RSG. This remained significant after adjusting for luminal space but not after correction for multiple testing. However, when only investigating the cancer samples (n=104), there were no significant differences in spermine concentrations between the RSGs. The reason for this discrepancy could be that the differences in concentrations are actually between cancer and benign tissue, and not the grades of RS. This would imply that the stromal-epithelial interaction does not affect spermine metabolism in the epithelial prostate cells. However, our results do not conflict with previous studies that have stated that cancer aggressiveness and spermine concentrations correlate. When analyzing which factors that were important for spermine concentration, we found GS to be highly significant ($p=7.6934E-05$), while tumor composition was irrelevant (table 7.4). It is an interesting observation that benign epithelial volume did not affect spermine concentration significantly in our samples, even though other studies have shown this correlation [51].

5.3.3 Choline and Choline Containing Compounds

ChoCC are important in phospholipid metabolism and cell membrane synthesis. Hence, they are important in cell proliferation regarding cancer progression [40]. No significant differences in none of the ChoCC concentrations were found when correlating them to RSG. For choline neither GS nor tumor composition were found to have a significant influence on its concentration (table 7.4). Nevertheless, looking at the initial mean concentrations (table 4.3) and the boxplots below (figure 5.1), the level of choline seems to have a visual apparent rise with increasing RSG and GS, though this was not confirmed

in the statistical analyses. These results are similar to Giskeodegard et al., who found differences in choline concentrations between cancer and no-cancer samples, but no significant changes regarding GS and tumor aggressiveness [23]. However, other studies have been able to confirm the correlation between choline concentration and GS [50, 75]. Keshari et al. found that the level of ChoCC, especially PC and GPC, and ethanol containing metabolites were significantly altered in high grade PCa compared to low grade. More interesting regarding our study is that they also found significant differences between phospholipid metabolisms in cultured human PCa cells *versus* intact PCa tissue [50]. This difference can be explained by the lack of epithelial-stromal interactions in cultured PCa cells, and it strengthens the impression of the importance of tumor microenvironment for PCa development and progression [50]. It also demonstrates the value of assessing entire human tissue samples, and not only the cancer cells independently.

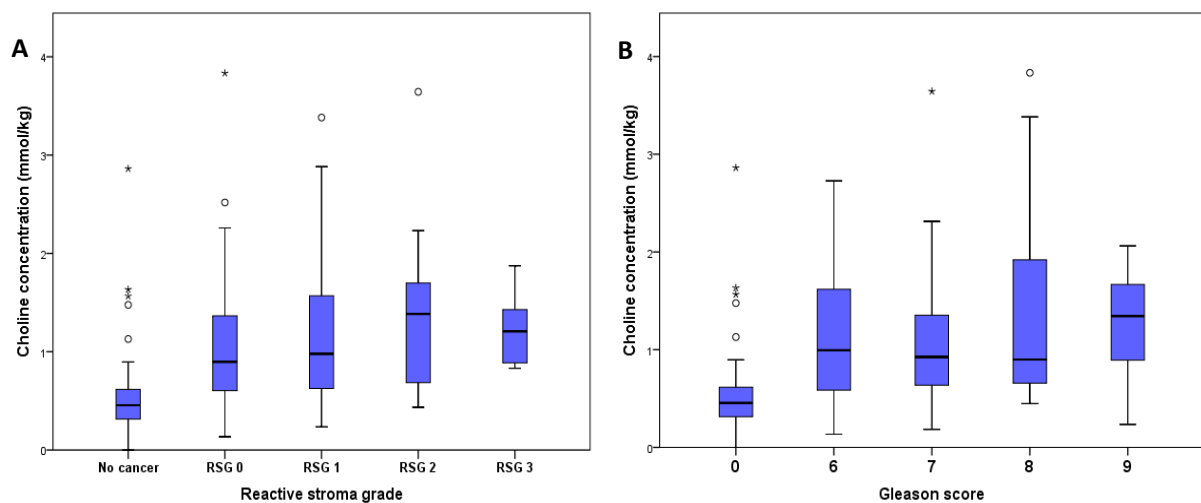


Figure 5.1: (A) Boxplot of choline concentrations for each RSG. (B) Boxplot of choline concentration for each GS.

5.4 Correction for Multiple Testing

The initial tests regarding RSG and citrate concentrations showed a significant correlation. However, after adjusting for multiple testing, using the Benjamini-Hochberg false discovery rate correction, the p-values became non-significant. We chose to present both the adjusted and initial p-values, because correction for multiple testing is an ongoing, highly discussed theme that we will address here.

When testing several hypotheses simultaneously, the risk of rejecting a true null hypothesis (type 1 error) increases. This is called the problem of multiplicity [76, 77]. The risk of getting significant results by chance increases with the number of tests performed and we tested 23 metabolites in several different combinations with LMM. Hence, there is a possibility that the significant differences we found

are not due to a true correlation between RSG and metabolite concentration, but purely by chance. Because of this problem, several methods to correct for multiple testing have been developed. These corrections take in account the number of tests performed. The BH correction adjusted the p-values upwards, so that $p=0.05$ still could be used as a threshold for significance. The adjusted p-values were computed from a FDR, which is the expected proportion of falsely rejected null hypotheses [71, 78]. Another method of multiple testing correction is the widely used Bonferroni correction. This method divides the threshold for significance by the number of tests performed. The new threshold is much lower and is applied for each individual test. [78]. As a result, the risk of false positive results decreases. Because correction for multiple testing decreases the risk of a type I errors, it becomes more difficult to obtain significant p-values when there actually is a true difference, and the chance of type II errors (failure to reject a false null hypothesis) increases [77].

In many multiple testing settings, the correction is too strict, making it almost impossible to reject the null hypothesis. Therefore, some researchers recommend using multiple testing correction with caution. Some even advise against it completely. When evaluating significance it is important not only to consider the p-value, but also the magnitude of effect and the quality of the study [77]. In addition, the consequence of a type I or type II errors should be taken in account when discussing whether or not correction for multiple testing should be performed [77].

A solution to the problem of multiplicity is to keep the number of tests as low as possible. This can be achieved by restricting the amount of end points tested, and thereby only testing what is specified in the hypothesis [76]. In our case, we tested all of the metabolites, not knowing exactly what information this would reveal. An alternative would have been to only test citrate, because this metabolite has shown importance in other studies. Then, correction for multiple testing would not have been necessary and our primary p-value would be representative, making our result significant. However, because we tested all of the 23 metabolites, we had to take in account the risk of obtaining significant results by chance. Because we already know citrate to be important in cancer metabolism, the multiple correction, in our case, might be too strict. The fact that citrate was the metabolite that singled out did not come as a surprise considering current knowledge. Therefore, we have presented the uncorrected p-values, so that the reader independently can evaluate the results.

5.5 Strengths and Limitations

The new standardized harvesting method, developed by Bertilsson et al. and applied by Giskeodegard et al., is an important strength of our study. By investigating HES-slices of tissue adjacent to the fresh frozen prostate slice, information about tissue content could be estimated accurately. Additionally, the precise location of core biopsies was determined, which lead to a considerably higher cancer content in the tissue samples used in our study (69,8% of the samples contained cancer) than what is possible to achieve with TRUS guided prostate biopsies. The HES-stained cryosections that were evaluated with histopathology were cut from the same sample that were used to obtain metabolic concentrations with HR-MAS. Hence, the pathologist's grading of RSG, GS and tissue content, could be directly linked to the metabolic spectra. The entire prostate slice was snap frozen on average 15 minutes after prostatectomy and both the core biopsies and later the cryosections, are obtained without thawing [74]. Thereby molecular degradation was kept at a minimum and the metabolite concentrations from HR-MAS were as representable for live prostate tissue as possible. Another important advantage of the harvesting method is that it does not interfere with routine histopathological evaluation of the surgically removed prostate. Also, Bertilsson et al. have proven that the tissues RNA is still highly intact after HR-MAS analyses. This shows that both genetic, metabolic and histopathological information can be obtained from the same tissue sample [74].

Another important strength of this study is the attention to inpatient correlations regarding metabolite concentration. This inpatient association can affect the relationship between histological observations and metabolite concentrations, leading to either false positive or false negative results. Because the number of samples obtained from each patient varied, some patients could have greater effect on the statistical analyses than others. However, by choosing LMM as the statistical model to analyze our data and adding the patient variable as a random effect, this inpatient correlation was accounted for. Thereby the model was able to separate the individual influence of patients from the real correlation between metabolite concentrations and RSG.

There are however some limitations to consider when evaluating this study. First, the histopathological evaluation of our HES slices can constitute an issue. As the core biopsies were frozen, the HES-slices cut from them were cryosections. Cryoslices can be difficult to evaluate as the cells appear smeared and the nucleoli blurred or even absent. However, pathologist Elin Richardsen assured us that even though the grading of RS was challenging, it was manageable. Second, the benign tissue samples in the study were obtained from patients with PCa in other areas of the prostate. It is not clear if, and how,

this might affect the metabolic concentrations acquired from these specimens. To avoid any unwanted interference it would have been desirable, but probably not ethically justifiable, to obtain benign samples from healthy prostate tissue. A possibility could be to use TURP samples from patients with BPH.

Finally, the number of tissue samples used in this study is small (n=149). Mostly, only the samples that contained cancer were used in our analyses, thereby reducing the dataset further (n=104). Only 6 tissue samples contained RSG 3, which is the most interesting RSG to investigate. The tissue samples were acquired by Bertillsson et al. and Giskeodegard et al. and their focus was on cancer aggressiveness and GS. Therefore, the HR-MAS samples were selected with respect to tumor content and GS, while RSG was first graded in the cryosections later. Therefore, the percentage of RS is small in comparison to other components. The small size of the dataset constitutes a problem for LMM analyses as well. Even though there were few samples, many factors had to be adjusted for. This divided the dataset in even smaller compartments, making it difficult to obtain significant results. In addition, one mistake by the pathologist when grading the tissue sample has much more effect on the results obtained from a small dataset than a bigger one. Therefore, a study with a larger amount of data, and especially more tissue samples containing RSG 2 and 3, could be able to reveal more information about the metabolic changes accompanying RS.

5.6 Clinical Translation

Because PCa is such a heterogeneous cancer, diagnostics and prognostics are often difficult. The multifocal growth makes biopsies uncertain as the GS is often underestimated because representative tissue is not sampled and evaluated. In addition, growing usage of PSA testing has increased the detection of indolent PCa, but at the same time, the positive consequences of detecting aggressive cancer in an early stage needs to be considered. However, PSA lacks both sensitivity and specificity leading to high numbers of false positive and false negative results. GS, PSA and the TNM system are used to risk stratify the patients and to choose the course of treatment, but this is often uncertain, especially with medium risk patients. Today's methods are therefore not able to separate indolent from aggressive cancer in a sufficient way. We need additional tools to better predict the nature of PCa, and to give the patients the treatment that provides them the best quality of life.

Reactive stroma has been proven to have prognostic value, independent of other factors such as GS and PSA [17, 18, 33]. This has been shown in both prostatectomies [18] and needle biopsies [17, 33].

Grading of RS can be performed on HES stained biopsy samples [17], and therefore the method could easily be implemented in today's diagnostic histological evaluation. Because GS only considers epithelial architecture, the practitioner needs to sample the area with the highest GS to do a correct risk stratification. As mentioned, the multifocal growth of PCa makes this difficult. Implementing RS in the evaluation could give additional information about tumor aggressiveness, even if the obtained samples do not contain the most representative epithelial area of the cancer. RSG 3 is the grade that holds the most novel predictive information, as this grade can be found within all GSs [18].

Metabolic profiling also has the potential of being implemented in routine diagnostics using MRS techniques. Several metabolite concentrations have been found to be able to discriminate between cancer and benign tissue [23]. Among these are citrate, spermine, lactate and alanine [23, 42, 51]. In addition, the concentrations of citrate and spermine have been shown to be significantly different in high grade ($GS \geq 7$) and low grade ($GS=6$) cancer, and are correlated to GS and tumor aggressiveness in prostatectomy samples [23]. Further, the CCP/C ratio is significantly altered in high-grade tumors compared to low grade [23, 61].

In diagnostic biopsies, it could be possible to use *ex vivo* HR-MAS to produce a metabolic profile of the sample, and therefore obtain a more accurate and detailed evaluation of the tumor. The CCP/C-ratio has been found to correlate in spatially matched *in vivo* MRS and *ex vivo* HR MAS, which proved that *ex-vivo* procedures adequately give information about the true *in vivo* metabolic profile [41]. Further, Giskeodegard et al. found that tissue composition had no influence on the metabolic concentrations of citrate and spermine [23]. We obtained the same result considering citrate, which was dependent only of RSG, GS and luminal space. This implies that the metabolic concentration of citrate changes only with PCa aggressiveness, independent of tumor volume. Consequently, HR-MAS examinations do not require the same precision in sampling as the histopathological evaluation, where it is important to extract the most representative tumor foci. HR-MAS could also be performed after prostatectomy, to control the initial risk evaluation, making a more reliable plan for adjuvant treatment and follow-up. The novel method for tissue harvesting, described by Bertilsson et al. [74], posts as a standardized method for obtaining high quality samples from prostatectomies. These samples can in addition to HR-MAS, be used for RNA extraction in genetic analyses and histopathological evaluation. Today, HR-MAS is mostly applied in research, but in the future of personalized medicine, this might be standard procedure for all patients.

The use of *in vivo* MRSI is a promising field. This non-invasive procedure can be of value in diagnostics, treatment evaluation and follow up of patients. Because previous mentioned metabolites have been found to correlate with GS, it is possible to use *in vivo* techniques to map cancer aggressiveness and discover PCa that does not manifest itself by PSA or DRE (figure 5.2). A metabolic map can also offer guidance when taking biopsies, thus increasing the probability of sampling the most representative areas [61]. Because MRSI can separate high and low grade tumors, it could be helpful when choosing the course of treatment, especially to select cases where active surveillance is sufficient [61].

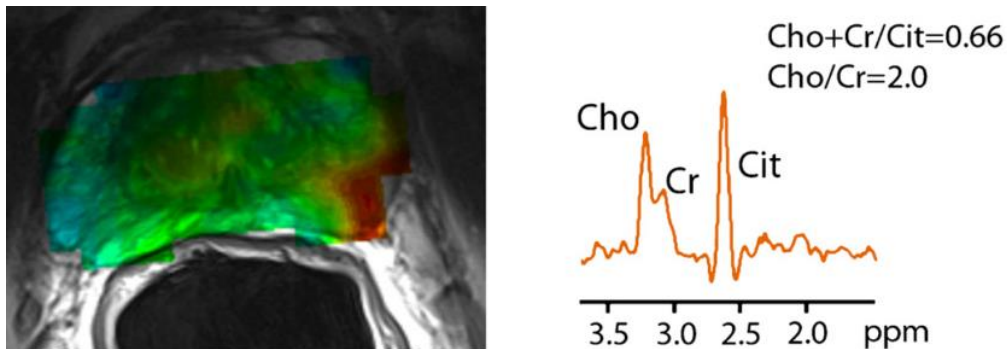


Figure 5.2: To the left, a metabolic map that shows the distribution of the (Choline+Creatine)/Citrate- ratio, indicating the most aggressive areas of the PCa. To the right, an example of a metabolic spectrum with the metabolites used in the ratio. The illustration is obtained from Kobus et al. [61].

Our study has focused on the correlation between metabolic concentrations and RS. Altered concentrations in different RSGs would strengthen the impression of stroma as an active participator in cancer development that needs to be taken in account. When evaluating cancer aggressiveness, both RS and metabolic profiles can separately provide valuable diagnostic information. Whether the combination of these two fields is promising is still unclear, and further research on the stromal-epithelial interactions in cancer development is necessary. Specific interactions need to be identified to fully understand the role and effect of RS. Hopefully, genetic analyses can reveal further information about the intricate mechanisms of cancer stroma. A goal for the future would be to identify interactions that could be targeted in therapy. From a more present perspective the trend towards different metabolic profiles between RSGs implies that MRSI and HR-MAS have the possibility to be used in a more extensive way, both in diagnostics, treatment and follow-up of PCa.

6 Conclusion

The results showed citrate concentration to be significantly correlated with RSG before correction for multiple testing. Citrate has previously been proven to have a negative correlation with tumor aggressiveness. However, GS and tumor volume were adjusted for in our model and therefore, the RSG can be considered as an independent factor for citrate concentration. This strengthens the impression of epithelial-stromal interactions as an active contributor in cancer development and progression. However, because the results did not remain significant after correction for multiple testing, it is not possible to confirm the correlation between RSG and citrate concentration. Further, it is possible to discuss whether a correction for multiple testing was necessary in this case, or if the correction may have led to a type II error. Regardless, the association between RSG and citrate concentration is interesting and needs further investigation. Both RS and MRS have the potential of being implemented in routine diagnostics, and their significance has already been proven in other studies. The more information we obtain, the closer we are to give each patient a precise diagnosis and risk evaluation, and further assure a targeted treatment and the best quality of life possible.

7 Appendix

Table 7.1: p-values for the correlation between metabolite concentrations and RSG adjusted for various fixed effects in cancer samples (n=104). Patient is added as random effect in all models. Not corrected for multiple testing.

Metabolite	Concentration ~ RS	Concentration ~ RS + GS	Concentration ~ RS + GS + tumor volume	Concentration ~ RS + GS + tumor volume + stromal volume
Choline	0.2410	0.2291	0.2047	0.1398
Creatine	0.6407	0.5893	0.5874	0.5941
Spermine	0.4222	0.1889	0.1880	0.2364
Putrescine*	0.2375	0.1881	0.1894	0.2370
Glycine	0.5171	0.4632	0.4407	0.4438
Glutamine	0.7941	0.8921	0.8433	0.8497
Glutamate	0.6087	0.4665	0.4127	0.4300
Ethanolamine*	0.0298	0.0232	0.0230	0.0373
Alanine	0.3464	0.3795	0.3678	0.3335
Valine	0.8358	0.9585	0.9628	0.9879
Taurine	0.7507	0.6715	0.6649	0.7263
Succinate	0.2256	0.2372	0.1833	0.1571
Scyllo-Inositol	0.2859	0.3108	0.3055	0.2794
Phosphoethanolamine	0.0704	0.0386	0.0388	0.0580
Phosphocholine*	0.1884	0.0998	0.1046	0.1691
Myo-Inositol	0.6670	0.6963	0.7056	0.6985
Leucine	0.3725	0.2325	0.1995	0.2011
Lactate	0.3832	0.3525	0.3458	0.3211
Isoleucine*	0.9179	0.8522	0.8535	0.7698
Glycerophosphocholine	0.2198	0.2332	0.2045	0.2086
Glycerophosphoethanol- amine*	0.0972	0.1188	0.1208	0.1330
Glucose*	0.0406	0.0471	0.0255	0.0100
Citrate	0.0308	0.0043	0.0044	0.0071

Significant p-values are marked in yellow. Borderline significant results are written in red.
*the metabolite is not normally distributed.

Table 7.2: p-values for the correlation between metabolite concentrations and RSG adjusted for various fixed effects in all samples (n=149). Patient is added as random effect in all models. Not corrected for multiple testing.

Metabolite	Concentration ~ RS	Concentration ~ RS + GS	Concentration ~ RS + GS + tumor volume	Concentration ~ RS + GS + tumor volume + stromal volume
Choline	1.3896E-7	0.3891	0.1854	0.1445
Creatine	0.9810	0.8152	0.7980	0.8425
Spermine	0.0894	0.0105	0.0129	0.0082
Putrescine*	0.0019	0.2086	0.1870	0.1891
Glycine	1.2186E-5	0.3522	0.1921	0.1885
Glutamine	2.1418E-5	0.4929	0.3791	0.3532
Glutamate	1.0031E-8	0.6238	0.4470	0.3958
Ethanolamine*	0.7970	0.0734	0.0652	0.0715
Alanine	0.0042	0.3370	0.2123	0.1616
Valine	0.0006	0.4971	0.4367	0.4267
Taurine	0.9408	0.2600	0.4245	0.4108
Succinate	0.0002	0.5685	0.3690	0.3181
Scyllo-Inositol	0.2190	0.7833	0.7428	0.7230
Phosphoethanolamine	2.6261E-5	0.0770	0.0819	0.0842
Phosphocholine*	5.3777E-5	0.0323	0.0249	0.0273
Myo-Inositol	0.3226	0.6908	0.7449	0.7525
Leucine	4.9774E-6	0.0744	0.0436	0.0381
Lactate	0.0001	0.7480	0.5943	0.5605
Isoleucine*	0.0040	0.7246	0.7761	0.7510
Glycerophosphocholine	1.1558E-5	0.6868	0.3734	0.3187
Glycerophosphoethanol- amine*	0.54816	0.4390	0.3566	0.3671
Glucose*	1.8408E-9	0.4891	0.0987	0.0917
Citrate	0.3332	0.0002	0.0003	0.0002

Significant p-values are marked in yellow. Borderline significant results are written in red.
*the metabolite is not normally distributed.

Table 7.3: p-values for the correlation between metabolite concentrations and RS grade in all samples (n=149). Adjusted for GS, tumor and stroma percentage, and the random effect of patient.

Metabolite	p-value before BH	p-value after BH
Choline	0.1445	0.3954
Creatine	0.8425	0.8425
Spermine	0.0082	0.0938
Putrescine*	0.1890	0.3954
Glycine	0.1885	0.3954
Glutamine	0.3532	0.5452
Glutamate	0.3958	0.5452
Ethanolamine*	0.0715	0.3015
Alanine	0.1616	0.3954
Valine	0.4267	0.5452
Taurine	0.4108	0.5452
Succinate	0.3181	0.5452
Scyllo-Inositol	0.7230	0.7867
Phosphoethanolamine	0.0842	0.3015
Phosphocholine*	0.0273	0.2092
Myo-Inositol	0.7525	0.7867
Leucine	0.0381	0.2191
Lactate	0.5605	0.6785
Isoleucine*	0.7510	0.7867
Glycerophosphocholine	0.3187	0.5452
Glycerophosphoethanolamine*	0.3671	0.5452
Glucose*	0.0917	0.3015
Citrate	1.5985E-4	0.0037

Significant p-values are marked in yellow. P-values that were significant before BH correction, but became non-significant after, are written in red.

*the metabolite does not have a normal distribution.

Table 7.4: p-values for the correlation between metabolite concentrations and each of the fixed effects implemented in the LMM.

Metabolite	RSG	GS	Tumor volume	Stroma volume
Choline	0.1398	0.9614	0.7064	0.1032
Creatine	0.5941	0.4423	0.8411	0.9984
Spermine	0.2364	6.1249E-05	0.4647	0.2632
Putrescine*	0.2370	0.1137	0.3328	0.2516
Glycine	0.4438	0.5728	0.1135	0.9771
Glutamine	0.8496	0.5980	0.0909	0.5728
Glutamate	0.4300	0.0930	0.0230	0.8772
Ethanolamine*	0.0373	0.2456	0.1125	0.1098
Alanine	0.3335	0.4159	0.4421	0.5826
Valine	0.9879	0.1442	0.6325	0.8142
Taurine	0.7263	0.2873	0.5526	0.5356
Succinate	0.1571	0.4226	0.2340	0.3744
Scyllo-Inositol	0.2794	0.8325	0.1712	0.5656
Phosphoethanolamine	0.0580	0.0188	0.2829	0.2692
Phosphocholine*	0.1691	0.1416	0.0620	0.1236
Myo-Inositol	0.6985	0.7553	0.9640	0.8836
Leucine	0.2011	0.0101	0.1518	0.8993
Lactate	0.3211	0.7128	0.5485	0.6468
Isoleucine*	0.7698	0.3190	0.2422	0.3285
Glycerophosphocholine	0.2086	0.4790	0.0993	0.9744
Glycerophosphoethanolamine*	0.1330	0.1680	0.8532	0.8067
Glucose*	0.0100	0.1010	0.7049	0.0121
Citrate	0.0071	2.0969E-06	0.2386	0.1890

Significant p-values are marked in yellow.
 *the metabolite is not normally distributed.

8 References

1. Tvetter, K. and R. Wahlqvist. *Prostata*. 2009 13.02.2009 [cited 2015 28. September]; Available from: <https://sml.snl.no/prostata>.
2. PubMed Health. *How does the prostate work?* 2012 [cited 28. September 23.10.12]; Available from: <http://www.ncbi.nlm.nih.gov/pubmedhealth/PMH0072475/>.
3. Urological Consultants of Florida. [cited 2015 15. October]; Picture of the prostate]. Available from: <http://www.miamiurologyconsultants.com/services-procedures/robotic-prostatectomy-surgery-prostate-cancer-miami-aventura-fl.php>.
4. IMU News. [cited 2015 15. October]; Available from: <http://imunews.imu.edu.my/health/1-6-men-diagnosed-prostate-cancer-every-man-know-2/>.
5. Lie, K. *Histologi ved prostatakreft*. 2013 [cited 2015 14. september]; Available from: <http://oncolex.no/Prostata/Bakgrunn/Histologi>.
6. Brennhovd, B. *Spredningsmønster for prostatakreft*. 2013 07.11.13 [cited 2015 28. september]; Available from: <http://oncolex.no/Prostata/Bakgrunn/Spredningsmonster>.
7. Cancerresearchuk.org. *Worldwide cancer incidence statistics 2014* [cited 2015 28. September]; Available from: <http://www.cancerresearchuk.org/health-professional/cancer-statistics/worldwide-cancer/incidence#heading-One>.
8. Solberg, A., et al., *Nasjonalt handlingsprogram med retningslinjer for diagnostikk, behandling og oppfølging av prostatakreft*. 3 ed. 2013: HelseDirektoratet 143.
9. Krefregisteret, *Cancer in Norway*. 2012.
10. Brennhovd, B. *Prostatakreft* 2013 07.11.2013 [cited 2015 28. September]; Available from: <http://oncolex.no/Prostata>.
11. Association of the Nordic Cancer Registries. [cited 2015 15. October]; Available from: <http://www.ancr.nu/ancr/>.
12. Løge, I. *Prostatakreft* 2014 22.06.2015 [cited 2015 14. september]; Available from: <http://legehandboka.no/mannlige-kjonnorgan/tilstander-og-sykdommer/prostata/prostatakreft-2402.html>.
13. Brennhovd, B. *Prostate cancer, diagnostics* 2013 07.11.2013 [cited 2015 03. september]; Available from: <http://oncolex.no/Prostata/Prosedyrekatolog/DIAGNOSTIKK?lg=procedureGroup>.
14. Wolf, A.M., et al., *American Cancer Society guideline for the early detection of prostate cancer: update 2010*. CA Cancer J Clin, 2010. **60**(2): p. 70-98.
15. Thue, G. *Prostate specific antigen, PSA*. 2013 [cited 2015 3. september.]; Available from: <http://legehandboka.no/laboratoriemedisin/medisinsk-biokjemi/blodprover/prostata-spesifikt-antigen-psa-3013.html>.
16. Eckersberger, E., et al., *Screening for Prostate Cancer: A Review of the ERSPC and PLCO Trials*. Rev Urol, 2009. **11**(3): p. 127-33.
17. Yanagisawa, N., et al., *Stromogenic prostatic carcinoma pattern (carcinomas with reactive stromal grade 3) in needle biopsies predicts biochemical recurrence-free survival in patients after radical prostatectomy*. Hum Pathol, 2007. **38**(11): p. 1611-20.
18. Ayala, G.E., et al., *Determining prostate cancer-specific death through quantification of stromogenic carcinoma area in prostatectomy specimens*. Am J Pathol, 2011. **178**(1): p. 79-87.
19. Harnden, P., et al., *Should the Gleason grading system for prostate cancer be modified to account for high-grade tertiary components? A systematic review and meta-analysis*. Lancet Oncol, 2007. **8**(5): p. 411-9.
20. Brennhovd, B. *Stadier ved prostatakreft*. 2013 [cited 2015 15. October]; Available from: <http://oncolex.no/Prostata/Bakgrunn/Stadier>.

21. Mottet, N., et al., *Guidelines on prostate cancer*. 2015: European association of Urology.
22. Arora, K. *Prostate*. [cited 2015 15. October]; Available from: <http://www.pathologyoutlines.com/topic/prostatestaging.html>.
23. Giskeodegard, G.F., et al., *Spermine and citrate as metabolic biomarkers for assessing prostate cancer aggressiveness*. PLoS One, 2013. **8**(4): p. e62375.
24. Brennhovd, B. *Behandling av prostatakreft* 2013 07.11.13 [cited 2015 28.09.2015]; Available from: <http://oncolex.no/Prostata/Prosedyre katalog/BEHANDLING?lg=procedureGroup>.
25. McDunn, J.E., et al., *Metabolomic signatures of aggressive prostate cancer*. *Prostate*, 2013. **73**(14): p. 1547-60.
26. Morgan, T., G. Palapattu, and J. Wei, *Screening for Prostate Cancer-Beyond Total PSA, Utilization of Novel Biomarkers*. *Curr Urol Rep*, 2015. **16**(9): p. 537.
27. Bjerklund, T.E. *Benign prostatahyperplasi (BPH)*. 2015 [cited 2015 14. september]; Available from: <http://legehandboka.no/mannlige-kjonnsorgan/tilstander-og-sykdommer/prostata/benign-prostatahyperplasi-2389.html>.
28. Draisma, G., et al., *Lead times and overdetection due to prostate-specific antigen screening: estimates from the European Randomized Study of Screening for Prostate Cancer*. *J Natl Cancer Inst*, 2003. **95**(12): p. 868-78.
29. Liu, Y., et al., *Prostate cancer - a biomarker perspective*. *Front Endocrinol (Lausanne)*, 2012. **3**: p. 72.
30. Kruslin, B., M. Ulamec, and D. Tomas, *Prostate cancer stroma: an important factor in cancer growth and progression*. *Bosn J Basic Med Sci*, 2015. **15**(2): p. 1-8.
31. Barron, D.A. and D.R. Rowley, *The reactive stroma microenvironment and prostate cancer progression*. *Endocr Relat Cancer*, 2012. **19**(6): p. R187-204.
32. Ayala, G., et al., *Reactive stroma as a predictor of biochemical-free recurrence in prostate cancer*. *Clin Cancer Res*, 2003. **9**(13): p. 4792-801.
33. Saeter, T., et al., *The prognostic value of reactive stroma on prostate needle biopsy: a population-based study*. *Prostate*, 2015. **75**(6): p. 662-71.
34. Billis, A., et al., *Adenocarcinoma on needle prostatic biopsies: does reactive stroma predicts biochemical recurrence in patients following radical prostatectomy?* *Int Braz J Urol*, 2013. **39**(3): p. 320-7.
35. Halama, A., *Metabolomics in cell culture--a strategy to study crucial metabolic pathways in cancer development and the response to treatment*. *Arch Biochem Biophys*, 2014. **564**: p. 100-9.
36. Exploring Research Biology. *What is metabolomics* Available from: <https://exploringresearchbio.wordpress.com/2013/04/16/what-is-metabolomics/>.
37. Kumar, V., A.K. Abbas, and J.C. Aster, *Robbins Basic Pathology* 9th ed. 2013: Eksevier Saunders
38. Costello, L.C. and R.B. Franklin, *'Why do tumour cells glycolyse?': from glycolysis through citrate to lipogenesis*. *Mol Cell Biochem*, 2005. **280**(1-2): p. 1-8.
39. Hanahan, D. and R.A. Weinberg, *Hallmarks of cancer: the next generation*. *Cell*, 2011. **144**(5): p. 646-74.
40. Bertilsson, H., et al., *Changes in gene transcription underlying the aberrant citrate and choline metabolism in human prostate cancer samples*. *Clin Cancer Res*, 2012. **18**(12): p. 3261-9.
41. Selnaes, K.M., et al., *Spatially matched in vivo and ex vivo MR metabolic profiles of prostate cancer -- investigation of a correlation with Gleason score*. *NMR Biomed*, 2013. **26**(5): p. 600-6.
42. Tessem, M.B., et al., *Evaluation of lactate and alanine as metabolic biomarkers of prostate cancer using 1H HR-MAS spectroscopy of biopsy tissues*. *Magn Reson Med*, 2008. **60**(3): p. 510-6.
43. Moestue, S., et al., *HR MAS MR spectroscopy in metabolic characterization of cancer*. *Curr Top Med Chem*, 2011. **11**(1): p. 2-26.

44. Mycielska, M.E., et al., *Citrate transport and metabolism in mammalian cells: prostate epithelial cells and prostate cancer*. *Bioessays*, 2009. **31**(1): p. 10-20.
45. Singh, K.K., et al., *Mitochondrial aconitase and citrate metabolism in malignant and nonmalignant human prostate tissues*. *Mol Cancer*, 2006. **5**: p. 14.
46. Costello, L.C. and R.B. Franklin, *The clinical relevance of the metabolism of prostate cancer; zinc and tumor suppression: connecting the dots*. *Mol Cancer*, 2006. **5**: p. 17.
47. Choi, S.Y., et al., *Cancer-generated lactic acid: a regulatory, immunosuppressive metabolite?* *J Pathol*, 2013. **230**(4): p. 350-5.
48. Awwad, H.M., J. Geisel, and R. Obeid, *The role of choline in prostate cancer*. *Clin Biochem*, 2012. **45**(18): p. 1548-53.
49. Glunde, K., Z.M. Bhujwalla, and S.M. Ronen, *Choline metabolism in malignant transformation*. *Nat Rev Cancer*, 2011. **11**(12): p. 835-48.
50. Keshari, K.R., et al., *Correlation of phospholipid metabolites with prostate cancer pathologic grade, proliferative status and surgical stage - impact of tissue environment*. *NMR Biomed*, 2011. **24**(6): p. 691-9.
51. Cheng, L.L., et al., *Non-destructive quantitation of spermine in human prostate tissue samples using HRMAS 1H NMR spectroscopy at 9.4 T*. *FEBS Letters*, 2001. **494**(1-2): p. 112-116.
52. van der Graaf, M., et al., *Proton MR spectroscopy of prostatic tissue focused on the detection of spermine, a possible biomarker of malignant behavior in prostate cancer*. *Magma*, 2000. **10**(3): p. 153-9.
53. Miller-Fleming, L., et al., *Remaining Mysteries of Molecular Biology: The Role of Polyamines in the Cell*. *J Mol Biol*, 2015.
54. Takyi, E.E., et al., *Deoxyribonucleic acid and polyamine synthesis in rat ventral prostate. Effects of age of the intact rat and androgen stimulation of the castrated rat with testosterone, 5 alpha-dihydrotestosterone and 5 alpha-androstane-3 beta, 17 beta-diol*. *Biochem J*, 1977. **162**(1): p. 87-97.
55. Shukla-Dave, A., et al., *Detection of prostate cancer with MR spectroscopic imaging: an expanded paradigm incorporating polyamines*. *Radiology*, 2007. **245**(2): p. 499-506.
56. Bakken, I.J., et al., *[In vivo magnetic resonance spectroscopy]*. *Tidsskr Nor Laegeforen*, 2002. **122**(14): p. 1365-8.
57. Gribbestad, I.S., et al. *Klinisk MR spektroskopi 2007* [cited 2015 2. september]; Available from: https://www.ntnu.no/c/document_library/get_file?uuid=47b1fcac-b2ad-40b7-8242-0890e1837bf1&groupId=10268.
58. Santos, C.F., et al., *Metabolic, pathologic, and genetic analysis of prostate tissues: quantitative evaluation of histopathologic and mRNA integrity after HR-MAS spectroscopy*. *NMR Biomed*, 2010. **23**(4): p. 391-8.
59. Fütterer, J.J., et al., *Standardized threshold approach using three-dimensional proton magnetic resonance spectroscopic imaging in prostate cancer localization of the entire prostate*. *Invest Radiol*, 2007. **42**(2): p. 116-22.
60. Swanson, M.G., et al., *Proton HR-MAS spectroscopy and quantitative pathologic analysis of MRI/3D-MRSI-targeted postsurgical prostate tissues*. *Magn Reson Med*, 2003. **50**(5): p. 944-54.
61. Kobus, T., et al., *In vivo assessment of prostate cancer aggressiveness using magnetic resonance spectroscopic imaging at 3 T with an endorectal coil*. *Eur Urol*, 2011. **60**(5): p. 1074-80.
62. Swanson, M.G., et al., *Quantitative analysis of prostate metabolites using 1H HR-MAS spectroscopy*. *Magn Reson Med*, 2006. **55**(6): p. 1257-64.
63. Opstad, K.S., et al., *Toward accurate quantification of metabolites, lipids, and macromolecules in HRMAS spectra of human brain tumor biopsies using LCMoDel*. *Magn Reson Med*, 2008. **60**(5): p. 1237-42.
64. Provencher, S.W., *Automatic quantitation of localized in vivo 1H spectra with LCMoDel*. *NMR Biomed*, 2001. **14**(4): p. 260-4.

65. Wright, A.J., et al., *Ex-vivo HRMAS of adult brain tumours: metabolite quantification and assignment of tumour biomarkers*. *Mol Cancer*, 2010. **9**: p. 66.
66. Provencher, S.W., *Estimation of metabolite concentrations from localized in vivo proton NMR spectra*. *Magn Reson Med*, 1993. **30**(6): p. 672-9.
67. Opstad, K.S., et al., *Correlations between in vivo (1)H MRS and ex vivo (1)H HRMAS metabolite measurements in adult human gliomas*. *J Magn Reson Imaging*, 2010. **31**(2): p. 289-97.
68. Seltman, H.J., *Experimental Design and Analysis*. 2015: <http://www.stat.cmu.edu/>.
69. Winter, B. University of California.
70. McDonald, J.H. 2014 2015 [cited 2015 19. October]; Available from: <http://www.biostathandbook.com/multiplecomparisons.html>.
71. Benjamini, Y. and Y. Hochberg, *Controlling the false discovery rate: a practical and powerful approach to multiple testing* *Journal of the royal statistical society*, 1995. **57**(1).
72. Silicon Genetics. 2003 [cited 2015 19. October]; Available from: http://physiology.med.cornell.edu/people/banfelder/qbio/resources_2008/1.5_Genespring_MTC.pdf.
73. Maltezos, S. and J. Horder. *Glutamate/glutamine and neuronal integrity in adults with ADHD: a proton MRS study*. 2015 [cited 2015 03. November]; Available from: Glutamate/glutamine and neuronal integrity in adults with ADHD: a proton MRS study.
74. Bertilsson, H., et al., *A new method to provide a fresh frozen prostate slice suitable for gene expression study and MR spectroscopy*. *Prostate*, 2011. **71**(5): p. 461-9.
75. van Asten, J.J., et al., *High resolution magic angle spinning NMR spectroscopy for metabolic assessment of cancer presence and Gleason score in human prostate needle biopsies*. *Magma*, 2008. **21**(6): p. 435-42.
76. Streiner, D.L. and G.R. Norman, *Correction for multiple testing: is there a resolution?* *Chest*, 2011. **140**(1): p. 16-8.
77. Feise, R.J., *Do multiple outcome measures require p-value adjustment?* *BMC Med Res Methodol*, 2002. **2**: p. 8.
78. Noble, W.S., *How does multiple testing correction work?* *Nat Biotechnol*, 2009. **27**(12): p. 1135-7.